# X 5    Quantum Theory of Molecular Magnetism

Jürgen Schnack

Fachbereich Physik

Universität Osnabrück

# Contents

# 1   Introduction

The synthesis of molecular magnets has undergone rapid progress in recent years [1, 2, 3, 4, 5, 6]. Each of the identical molecular units can contain as few as two and up to several dozens of paramagnetic ions ("spins"). One of the largest paramagnetic molecules synthesized to date, the polyoxometalate $\{Mo_{72}Fe_{30}\}$ [7] contains 30 iron ions of spin $s = 5/2$. Although these materials appear as macroscopic samples, i. e. crystals or powders, the intermolecular magnetic interactions are utterly negligible as compared to the intramolecular interactions. Therefore, measurements of their magnetic properties reflect mainly ensemble properties of single molecules.

Their magnetic features promise a variety of applications in physics, magneto-chemistry, biology, biomedicine and material sciences [1, 3, 4] as well as in quantum computing [8, 9, 10]. The most promising progress so far is being made in the field of spin crossover substances using effects like "Light Induced Excited Spin State Trapping (LIESST)" [11].

It appears that in the majority of these molecules the localized single-particle magnetic moments couple antiferromagnetically and the spectrum is rather well described by the Heisenberg model with isotropic nearest neighbor interaction sometimes augmented by anisotropy terms [12, 13, 14, 15, 16]. Thus, the interest in the Heisenberg model, which is known already for a long time [17], but used mostly for infinite one-, two-, and three-dimensional systems, was renewed by the successful synthesis of magnetic molecules. Studying such spin arrays focuses on qualitatively new physics caused by the finite size of the system.

Several problems can be solved with classical spin dynamics, which turns out to provide accurate quantitative results for static properties, such as magnetic susceptibility, down to thermal energies of the order of the exchange coupling. However, classical spin dynamics will not be the subject of this chapter, it is covered in many publications on Monte-Carlo and thermostated spin dynamics. One overview article which discusses classical spin models in the context of spin glasses is given by Ref. [18].

Theoretical inorganic chemistry itself provides several methods to understand and describe molecular magnetism, see for instance Ref. [19]. In this chapter we would like to focus on those subjects which are of general interest in the context of this book.

# 2   Substances

From the viewpoint of theoretical magnetism it is not so important which chemical structures magnetic molecules actually have. Nevertheless, it is very interesting to note that they appear in almost all branches of chemistry. There are inorganic magnetic molecules like polyoxometalates, metal-organic molecules, and purely organic magnetic molecules in which radicals carry the magnetic moments. It is also fascinating that such molecules can be synthesized in a huge variety of structures extending from rather unsymmetric structures to highly symmetric rings.

One of the first magnetic molecules to be synthesized was Mn-12-acetate [20] ($Mn_{12}$) – [$Mn_{12}O_{12}(CH_3COO)_{16}(H_2O)_4$] – which by now serves as the "drosophila" of molecular magnetism, see e. g. [1, 21, 4, 22, 23]. As shown in Fig. 1 the molecules contains four Mn(IV) ions ($s = 3/2$) and eight Mn(III) ions ($s = 2$) which are magnetically coupled to give an $S = 10$ ground state. The molecules possesses a magnetic anisotropy, which determines the observed relaxation of the magnetization and quantum tunneling at low temperatures [21, 24].

Although the investigation of magnetic molecules in general – and of Mn-12-acetate in partic-
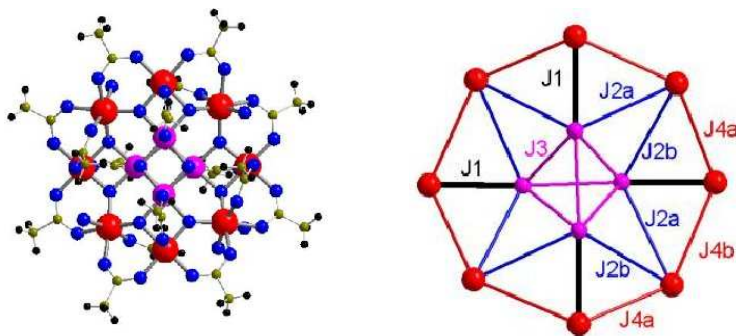
**Fig. 1:** *Structure of Mn-12-acetate: On the l.h.s. the Mn ions are depicted by large spheres, on the r.h.s. the dominant couplings are given. With friendly permission by G. Chaboussant.*

ular – has made great advances over the past two decades, it is still a challenge to deduce the underlying microscopic Hamiltonian, even if the Hamiltonian is of Heisenberg type. Mn-12-acetate is known for about 20 years now and investigated like no other magnetic molecule, but only recently its model parameters could be estimated with satisfying accuracy [25, 26].
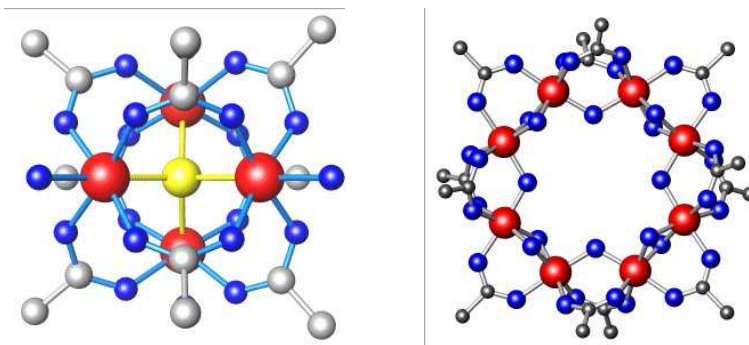


**Fig. 2:** *Structure of a chromium-4 and a chromium-8 ring. The Cr ions are depicted by large spheres.*

Another very well investigated class of molecules is given by spin rings among which iron rings ("ferric wheels") are most popular [27, 28, 29, 30, 31, 32, 33, 34]. Iron-6 rings for instance can host alkali ions such as lithium or sodium which allows to modify the parameters of the spin Hamiltonian within some range [16, 35]. Another realization of rings is possible using chromium ions as paramagnetic centers. Figure 2 shows the structure of two rings, one with four chromium ions the other one with eight chromium ions.

A new route to molecular magnetism is based on so-called Keplerate structures which allow the synthesis of truly giant and highly symmetric spin arrays. The molecule $\{Mo_{72}Fe_{30}\}$ [7, 36] containing 30 iron ions of spin $s = 5/2$ may be regarded as the archetype of such structures. Figure 3 shows on the l.h.s. the inner skeleton of this molecule – Fe and O-Mo-O bridges – as well as the classical ground state [37] depicted by arrows on the r.h.s. [36].

One of the obvious advantages of magnetic molecules is that the magnetic centers of different molecules are well separated by the ligands of the molecules. Therefore, the intermolecular interactions are utterly negligible and magnetic molecules can be considered as being independent. Nevertheless, it is desirable to build up nanostructured materials consisting of magnetic molecules in a controlled way. Figure 4 gives an example of a planar structure consisting of layers of $\{Mo_{72}Fe_{30}\}$ [38, 39] which has been synthesized recently together with a linear structure
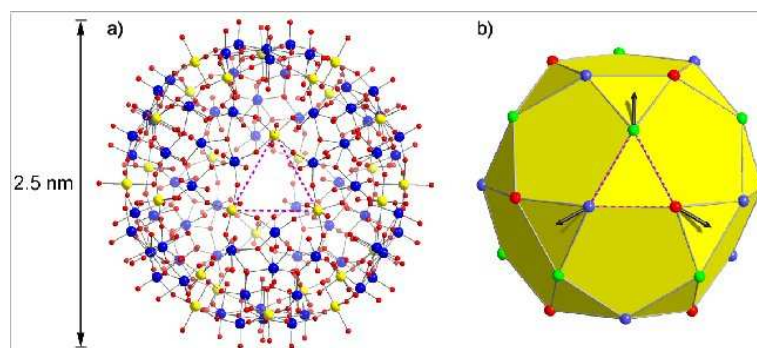
**Fig. 3:** *Structure of $\{Mo_{72}Fe_{30}\}$, a giant Keplerate molecule where 30 iron ions are placed at the vertices of an icosidodecahedron. L.h.s.: sketch of the chemical structure, r.h.s. magnetic structure showing the iron ions (spheres), the nearest neighbor interactions (edges) as well as the spin directions in the classical ground state. The dashed triangle on the l.h.s. corresponds to the respective triangle on the r.h.s.. With friendly permission by Paul Kögerler [36].*
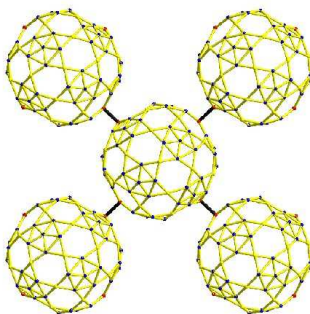


**Fig. 4:** *Square lattice of $\{Mo_{72}Fe_{30}\}$-molecules: Each molecule is connected with its four nearest neighbors by an antiferromagnetic coupling. With friendly permission by Paul Kögerler [38, 39].*

consisting of chains of $\{Mo_{72}Fe_{30}\}$ [40]. These systems show new combinations of physical properties that stem from both molecular and bulk effects.

Many more structures than those sketched above can be synthesized nowadays and with the increasing success of coordination chemistry more are yet to come. The final hope of course is that magnetic structures can be designed according to the desired magnetic properties. But this goal is not close at all, it requires further understanding of the interplay of magneto-chemistry and magnetic phenomena. One of the tools used to clarify such questions is density functional theory or other *ab initio* methods [41, 42, 43, 44, 45, 46].

# 3   Theoretical techniques and results

## 3.1   Hamiltonian

It appears that in the majority of these molecules the interaction between the localized single-particle magnetic moments can be rather well described by the Heisenberg model with isotropic (nearest neighbor) interaction and an additional anisotropy term [12, 13, 14, 15, 16]. Dipolar interactions are usually of minor importance. It is also found that antiferromagnetic interactions

are favored in most molecules leading to nontrivial ground states.

## Heisenberg Hamiltonian

For many magnetic molecules the total Hamilton operator can be written as

$$\underset{\sim}{H} = \underset{\sim}{H}_{\text{Heisenberg}} + \underset{\sim}{H}_{\text{anisotropy}} + \underset{\sim}{H}_{\text{Zeeman}} \tag{1}$$

$$\underset{\sim}{H}_{\text{Heisenberg}} = -\sum_{u,v} J_{uv} \underset{\sim}{\vec{s}}(u) \cdot \underset{\sim}{\vec{s}}(v) \tag{2}$$

$$\underset{\sim}{H}_{\text{anisotropy}} = -\sum_{u=1}^{N} d_u (\vec{e}(u) \cdot \underset{\sim}{\vec{s}}(u))^2 \tag{3}$$

$$\underset{\sim}{H}_{\text{Zeeman}} = g\mu_B \vec{B} \cdot \underset{\sim}{\vec{S}} . \tag{4}$$

The Heisenberg Hamilton operator[1] in the form given in Eq. (2) is isotropic, $J_{uv}$ is a symmetric matrix containing the exchange parameters between spins at sites $u$ and $v$. The exchange parameters are usually given in units of energy, and $J_{uv} < 0$ corresponds to antiferromagnetic, $J_{uv} > 0$ to ferromagnetic coupling[2]. The sum in (2) runs over all possible tuples $(u,v)$. The vector operators $\underset{\sim}{\vec{s}}(u)$ are the single-particle spin operators.

The anisotropy terms (3) usually simplify to a large extend, for instance for spin rings, where the site-dependent directions $\vec{e}(u)$ are all equal, e. g. $\vec{e}(u) = \vec{e}_z$ and the strength as well is the same for all sites $d_u = d$.

The third part (Zeeman term) in the full Hamiltonian describes the interaction with the external magnetic field. Without singe-site and $g$-value anisotropy the direction of the field can be assumed to be along the $z$-axis which simplifies the Hamiltonian very much.

Although the Hamiltonian looks rather simple, the eigenvalue problem is very often not solvable due to the huge dimension of the Hilbert space or because the number of exchange constants is too big to allow an accurate determination from experimental data. Therefore, one falls back to effective single-spin Hamiltonians for molecules with non-zero ground state spin and a large enough gap to higher-lying multiplets.

## Single-spin Hamiltonian

For molecules like $Mn_{12}$ and $Fe_8$ which possess a high ground state spin and well separated higher lying levels the following single-spin Hamiltonian

$$\underset{\sim}{H} = -D_2 \underset{\sim}{S}_z^2 - D_4 \underset{\sim}{S}_z^4 + \underset{\sim}{H}' \tag{5}$$

$$\underset{\sim}{H}' = g\mu_B B_x \underset{\sim}{S}_x \tag{6}$$

is appropriate, see e. g. Ref. [23]. The first two terms of the Hamilton operator $\underset{\sim}{H}$ represent the anisotropy whereas $\underset{\sim}{H}'$ is the Zeeman term for a magnetic field along the $x$-axis. The total spin is fixed, i. e. $S = 10$ for $Mn_{12}$ and $Fe_8$, thus the dimension of the Hilbert space is $\dim(\mathcal{H}) = 2S + 1$.

The effective Hamiltonian (5) is sufficient to describe the low-lying spectrum and phenomena like magnetization tunneling. Since $\underset{\sim}{H}'$ does not commute with the $z$-component of the total

---

[1]Operators are denoted by a tilde.

[2]One has to be careful with this definition since it varies from author to author

spin $\underset{\sim}{S}_z$, every eigenstate $|M\rangle$ of $\underset{\sim}{S}_z$, i. e. the states with good magnetic quantum number $M$, is not stationary but will tunnel through the barrier and after half the period be transformed into $|-M\rangle$.

## 3.2 Evaluating the spectrum

The ultimate goal is to evaluate the complete eigenvalue spectrum of the full Hamilton operator (1) as well as all eigenvectors. Since the total dimension of the Hilbert space is usually very large, e. g. $\dim(\mathcal{H}) = (2s+1)^N$ for a system of $N$ spins of equal spin quantum number $s$, a straightforward diagonalization of the full Hamilton matrix is not feasible. Nevertheless, very often the Hamilton matrix can be decomposed into a block structure because of spin symmetries or space symmetries. Accordingly the Hilbert space can be decomposed into mutually orthogonal subspaces. Then for a practical evaluation only the size of the largest matrix to be diagonalized is of importance (relevant dimension).

**Product basis**

The starting point for any diagonalization is the product basis $|\vec{m}\rangle = |m_1, \ldots, m_u, \ldots, m_N\rangle$ of the single-particle eigenstates of all $\underset{\sim}{s}_z(u)$

$$\underset{\sim}{s}_z(u)\,|m_1, \ldots, m_u, \ldots, m_N\rangle = m_u\,|m_1, \ldots, m_u, \ldots, m_N\rangle\,. \tag{7}$$

These states are sometimes called Ising states. They span the full Hilbert space and are used to construct symmetry-related basis states.

**Symmetries of the problem**

Since the isotropic Heisenberg Hamiltonian includes only a scalar product between spins, this operator is rotationally invariant in spin space, i. e. it commutes with $\vec{\underset{\sim}{S}}$ and thus also with $\underset{\sim}{S}_z$

$$\left[\underset{\sim}{H}_{\text{Heisenberg}}, \vec{\underset{\sim}{S}}^2\right] = 0 \quad , \qquad \left[\underset{\sim}{H}_{\text{Heisenberg}}, \underset{\sim}{S}_z\right] = 0\,. \tag{8}$$

In a case where anisotropy is negligible a well-adapted basis is thus given by the simultaneous eigenstates $|S, M, \alpha\rangle$ of $\vec{\underset{\sim}{S}}^2$ and $\underset{\sim}{S}_z$, where $\alpha$ enumerates those states belonging to the same $S$ and $M$ [47, 48]. Since the applied magnetic field can be assumed to point into $z$-direction for vanishing anisotropy the Zeeman term automatically also commutes with $\underset{\sim}{H}_{\text{Heisenberg}}$, $\vec{\underset{\sim}{S}}^2$, and $\underset{\sim}{S}_z$. Since $M$ is a good quantum number the Zeeman term does not need to be included in the diagonalization but can be added later.

Besides spin symmetries many molecules possess spatial symmetries. One example is given by spin rings which have a translational symmetry. In general the symmetries depend on the point group of the molecule; for the evaluation of the eigenvalue spectrum its irreducible representations have to be used [13, 16, 47]. Thus, in a case with anisotropy one looses spin rotational symmetries but one can still use space symmetries. Without anisotropy one even gains a further reduction of the relevant dimension.

## Dimension of the problem

The following section illuminates the relevant dimensions assuming certain symmetries[3].
If no symmetry is present the total dimension is just

$$\dim\left(\mathcal{H}\right) = \prod_{u=1}^{N} \left(2s(u) + 1\right) \tag{9}$$

for a spin array of $N$ spins with various spin quantum numbers. In many cases the spin quantum numbers are equal resulting in a dimension of the total Hilbert space of $\dim(\mathcal{H}) = (2s + 1)^N$.
If the Hamiltonian commutes with $\underset{\sim}{S}_z$ then $M$ is a good quantum number and the Hilbert space $\mathcal{H}$ can be divided into mutually orthogonal subspaces $\mathcal{H}(M)$

$$\mathcal{H} = \bigoplus_{M=-S_{\max}}^{+S_{\max}} \mathcal{H}(M)\,, \quad S_{\max} = \sum_{u=1}^{N} s(u)\,. \tag{10}$$

For given values of $M$, $N$ and of all $s(u)$ the dimension $\dim\left(\mathcal{H}(M)\right)$ can be determined as the number of product states (7), which constitute a basis in $\mathcal{H}(M)$, with $\sum_u m_u = M$. The solution of this combinatorial problem can be given in closed form [48]

$$\dim\left(\mathcal{H}(M)\right) = \frac{1}{(S_{\max} - M)!} \left[ \left(\frac{d}{dz}\right)^{S_{\max}-M} \prod_{x=1}^{N} \frac{1 - z^{2s(x)+1}}{1 - z} \right]_{z=0}. \tag{11}$$

For equal single-spin quantum numbers $s(1) = \cdots = s(N) = s$, and thus a maximum total spin quantum number of $S_{\max} = Ns$, (11) simplifies to

$$\dim\left(\mathcal{H}(M)\right) = f(N, 2s + 1, S_{\max} - M) \quad \text{with} \tag{12}$$

$$f(N, \mu, \nu) = \sum_{n=0}^{\lfloor \nu/\mu \rfloor} (-1)^n \binom{N}{n} \binom{N - 1 + \nu - n\mu}{N - 1}.$$

In both formulae (11) and (12), $M$ may be replaced by $|M|$ since the dimension of $\mathcal{H}(M)$ equals those of $\mathcal{H}(-M)$. $\lfloor \nu/\mu \rfloor$ in the sum symbolizes the greatest integer less or equal to $\nu/\mu$.
Eq. (12) is known as a result of de Moivre [49].
If the Hamiltonian commutes with $\vec{\underset{\sim}{S}}^2$ and all individual spins are identical the dimensions of the orthogonal eigenspaces $\mathcal{H}(S, M)$ can also be determined. The simultaneous eigenspaces $\mathcal{H}(S, M)$ of $\vec{\underset{\sim}{S}}^2$ and $\underset{\sim}{S}_z$ are spanned by eigenvectors of $\underset{\sim}{H}$. The one-dimensional subspace $\mathcal{H}(M = S_{\max}) = \mathcal{H}(S_{\max}, S_{\max})$, especially, is spanned by $|\,\Omega\,\rangle$, a state called magnon vacuum. The total ladder operators (spin rising and lowering operators) are

$$\underset{\sim}{S}^{\pm} = \underset{\sim}{S}_x \pm i\,\underset{\sim}{S}_y\,. \tag{13}$$

For $S > M$, $\underset{\sim}{S}^-$ maps any normalized $\underset{\sim}{H}$-eigenstate $\in \mathcal{H}(S, M + 1)$ onto an $\underset{\sim}{H}$-eigenstate $\in \mathcal{H}(S, M)$ with norm $\sqrt{S(S + 1) - M(M + 1)}$.
For $0 \le M < S_{\max}$, $\mathcal{H}(M)$ can be decomposed into orthogonal subspaces

$$\mathcal{H}(M) = \mathcal{H}(M, M) \oplus \underset{\sim}{S}^- \mathcal{H}(M + 1) \tag{14}$$

---

[3]Work done with Klaus Bärwinkel and Heinz-Jürgen Schmidt, Universität Osnabrück, Germany.

with

$$S^- \mathcal{H}(M+1) = \bigoplus_{S \geq M+1} \mathcal{H}(S,M) . \qquad (15)$$

In consequence, the diagonalization of $H$ in $\mathcal{H}$ has now been traced back to diagonalization in the subspaces $\mathcal{H}(S,S)$, the dimension of which are for $S < S_{\text{max}}$

$$\dim(\mathcal{H}(S,S)) = \dim(\mathcal{H}(M=S)) - \dim(\mathcal{H}(M=S+1)) \qquad (16)$$

and can be calculated according to (12).

As an example for space symmetries I would like to discuss the translational symmetry found in spin rings. The discussed formalism can as well be applied to other symmetry operations which can be mapped onto a translation. Any such translation is represented by the cyclic shift operator $T$ or a multiple repetition. $T$ is defined by its action on the product basis (7)

$$T \,|\, m_1, \ldots, m_{N-1}, m_N \rangle = |\, m_N, m_1, \ldots, m_{N-1} \rangle . \qquad (17)$$

The eigenvalues of $T$ are the $N$-th roots of unity

$$z_k = \exp\left\{-i\frac{2\pi k}{N}\right\} , \qquad k = 0, \ldots, N-1 , \qquad p_k = 2\pi k/N , \qquad (18)$$

where $k$ will be called translational (or shift) quantum number and $p_k$ momentum quantum number or crystal momentum. The shift operator $T$ commutes not only with the Hamiltonian but also with total spin. Any $\mathcal{H}(S,M)$ can therefore be decomposed into simultaneous eigenspaces $\mathcal{H}(S,M,k)$ of $\vec{S}^2$, $S_z$ and $T$.

In the following we demonstrate how an eigenbasis of both $S_z$ and $T$ can be constructed, this basis spans the orthogonal Hilbert spaces $\mathcal{H}(M,k)$. How total spin can be included by means of an irreducible tensor operator approach is described in Refs. [13, 16, 47].

A special decomposition of $\mathcal{H}$ into orthogonal subspaces can be achieved by starting with the product basis and considering the equivalence relation

$$|\psi\rangle \cong |\phi\rangle \Leftrightarrow |\psi\rangle = T^n \,|\phi\rangle , \, n \in \{1, 2, \ldots, N\} \qquad (19)$$

for any pair of states belonging to the product basis. The equivalence relation then induces a complete decomposition of the basis into disjoint subsets, i. e. the equivalence classes. A "cycle" is defined as the linear span of such an equivalence class of basis vectors. The obviously orthogonal decomposition of $\mathcal{H}$ into cycles is compatible with the decomposition of $\mathcal{H}$ into the various $\mathcal{H}(M)$. Evidently, the dimension of a cycle can never exceed $N$. Cycles are called "proper cycles" if their dimension equals $N$, they are termed "epicycles" else. One of the $N$ primary basis states of a proper cycle may arbitrarily be denoted as

$$|\psi_1\rangle = |\, m_1, \ldots, m_N \rangle \qquad (20)$$

and the remaining ones may be enumerated as

$$|\psi_{n+1}\rangle = T^n \,|\psi_1\rangle , \, n = 1, 2, \ldots, N-1 . \qquad (21)$$

The cycle under consideration is likewise spanned by the states

$$| \chi_k \rangle = \frac{1}{\sqrt{N}} \sum_{\nu=0}^{N-1} \left( e^{i\frac{2\pi k}{N}} \underset{\sim}{T} \right)^{\nu} | \psi_1 \rangle \tag{22}$$

which are eigenstates of $\underset{\sim}{T}$ with the respective shift quantum number $k$. Consequently, every $k$ occurs once in a proper cycle. An epicycle of dimension $D$ is spanned by $D$ eigenstates of $\underset{\sim}{T}$ with each of the translational quantum numbers $k = 0, N/D, \ldots, (D-1)N/D$ occurring exactly once.

As a rule of thumb one can say that the dimension of each $\mathcal{H}(M, k)$ is approximately $\dim(\mathcal{H}(M, k)) \approx \dim(\mathcal{H}(M))/N$. An exact evaluation of the relevant dimensions for spin rings can be obtained from Ref. [48].

## Exact diagonalization

If the relevant dimension is small enough the respective Hamilton matrices can be diagonalized, either analytically [50, 51, 48] or numerically, see e. g. [52, 53, 54, 55, 13, 56, 57, 47].

Again, how such a project is carried out, will be explained with the help of an example, a simple spin ring with $N = 6$ and $s = 1/2$. The total dimension is $\dim(\mathcal{H}) = (2s+1)^N = 64$. The Hamilton operator (2) simplifies to

$$\underset{\sim}{H}_{\text{Heisenberg}} = -2J \sum_{u=1}^{N} \vec{\underset{\sim}{s}}(u) \cdot \vec{\underset{\sim}{s}}(u+1) , \quad N+1 \equiv 1 . \tag{23}$$

We start with the magnon vacuum $| \Omega \rangle = | +++++ + \rangle$ which spans the Hilbert space $\mathcal{H}(M)$ with $M = Ns = 3$. "$\pm$" are shorthand notations for $m = \pm 1/2$. The dimension of the subspace $\dim(\mathcal{H}(M = Ns))$ is one and the energy eigenvalue is $E_\Omega = -2JNs^2 = -3J$. $| \Omega \rangle$ is an eigenstate of the shift operator with $k = 0$. Since $S$ is also a good quantum number in this example $| \Omega \rangle$ has to be an eigenstate of $\vec{\underset{\sim}{S}}^2$, too, the quantum number is $S = Ns$.

The next subspace $\mathcal{H}(M)$ with $M = Ns - 1 = 2$ is spanned by $| -+++++ \rangle$ and the five other vectors which are obtained by repetitive application of $\underset{\sim}{T}$. This subspace obviously has the dimension $N$, and the cycle spanned by $\underset{\sim}{T}^n | -+++++ \rangle, n = 0, \ldots, N-1$ is a proper one. Therefore, each $k$ quantum number arises once. The respective eigenstates of $\underset{\sim}{T}$ can be constructed according to Eq. (22) as

$$| M = 2, k \rangle = \frac{1}{\sqrt{N}} \sum_{\nu=0}^{N-1} \left( e^{i\frac{2\pi k}{N}} \underset{\sim}{T} \right)^{\nu} | -+++++ \rangle . \tag{24}$$

All subspaces $\mathcal{H}(M, k)$ have dimension one. Since $\underset{\sim}{S}^- | \Omega \rangle$ is a state belonging to $\mathcal{H}(M = Ns - 1)$ with the same $k$-quantum number as $| \Omega \rangle$ it is clear that $| M = 2, k = 0 \rangle$ is a already an eigenstate of $\vec{\underset{\sim}{S}}^2$ with $S = Ns$. The other $| M = 2, k \neq 0 \rangle$ must have $S = Ns - 1$.

The next subspace $\mathcal{H}(M)$ with $M = Ns - 2 = 1$ is spanned by three basic vectors, i. e. $| --++++ \rangle, | -+-+++ \rangle, | -++-++ \rangle$ and the repetitive applications of $\underset{\sim}{T}$ onto them. The first two result in proper cycles, the third vector $| -++-++ \rangle$ results in an epicycle of dimension three, thus for the epicycle we find only $k$ quantum numbers $k = 0, 2, 4$. The energy eigenvalues found in the subspace $\mathcal{H}(M = Ns - 1)$ ("above") must reappear here which

again allows to address an $S$ quantum number to these eigenvalues. The dimension of the subspace $\mathcal{H}(M = 1)$ is 15, the dimensions of the subspaces $\mathcal{H}(M, k)$ are 3 ($k = 0$), 2 ($k = 1$), 3 ($k = 2$), 2 ($k = 3$), 3 ($k = 4$), and 2 ($k = 5$).

The last subspace which has to be considered belongs to $M = 0$ and is spanned by $|---+++\rangle$, $|--+-++$ and repetitive applications of $\underset{\sim}{T}$. Its dimension is 20. Here $|-+-+-+\rangle$ leads to an epicycle of dimension two.

The Hamilton matrices in subspaces with $M < 0$ need not to be diagonalized due to the $\underset{\sim}{S_z}$-symmetry, i. e. eigenstates with negative $M$ can be obtained by transforming all individual $m_u \rightarrow -m_u$. Summing up the dimensions of all $\mathcal{H}(M)$ then yields $1+6+15+20+15+6+1 = 64 \ \checkmark$.
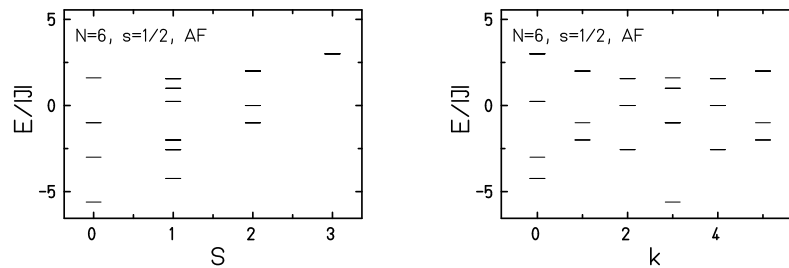


**Fig. 5:** *Energy eigenvalues as a function of total spin quantum number $S$ (l.h.s.) and $k$ (r.h.s.).*

Figure 5 shows the resulting energy spectrum both as a function of total spin $S$ as well as a function of translational quantum number $k$.

### Projection and Lanczos method

Complex hermitian matrices can be completely diagonalized numerically up to a size of about 10,000 by 10,000 which corresponds to about 1.5 Gigabyte of necessary RAM. Nevertheless, for larger systems one can still use numerical methods to evaluate low-lying energy levels and the respective eigenstates with high accuracy.

A simple method is the projection method [55] which rests on the multiple application of the Hamiltonian on some random trial state.

To be more specific let's approximate the ground state of a spin system. We start with a random trial state $|\phi_0\rangle$ and apply an operator which "cools" the system. This operator is given by the time evolution operator with imaginary time steps

$$|\tilde{\phi}_1\rangle \;=\; \exp\left\{-\varepsilon\underset{\sim}{H}\right\} |\phi_0\rangle . \qquad (25)$$

Expanding $|\phi_0\rangle$ into eigenstates $|\nu\rangle$ of the Hamilton operator elucidates how the method works

$$|\tilde{\phi}_1\rangle \;=\; \sum_{\nu=0} \exp\left\{-\varepsilon E_\nu\right\} |\nu\rangle\langle\nu|\phi_0\rangle \qquad (26)$$

$$=\; \exp\left\{-\varepsilon E_0\right\} \sum_{\nu=0} \exp\left\{-\varepsilon(E_\nu - E_0)\right\} |\nu\rangle\langle\nu|\phi_0\rangle . \qquad (27)$$

Relative to the ground state component all other components are exponentially suppressed. For

practical purposes equation (26) is linearized and recursively used

$$| \tilde{\phi}_{i+1} \rangle = \left( 1 - \varepsilon \underset{\sim}{H} \right) | \phi_i \rangle , \quad | \phi_{i+1} \rangle = \frac{| \tilde{\phi}_{i+1} \rangle}{\sqrt{\langle \tilde{\phi}_{i+1} | \tilde{\phi}_{i+1} \rangle}} . \tag{28}$$

$\varepsilon$ has to be small enough in order to allow the linearization of the exponential. It is no problem to evaluate several higher-lying states by demanding that they have to be orthogonal to the previous ones. Restricting the calculation to orthogonal eigenspaces yields low-lying states in these eigenspaces which allows to evaluate even more energy levels. The resulting states obey the properties of the Ritz variational principle, i. e. they lie above the ground state and below the highest one.

Another method to partially diagonalize a huge matrix was proposed by Cornelius Lanczos in 1950 [58, 59]. Also this method uses a (random) initial vector. It then generates an orthonormal system in such a way that the representation of the operator of interest is tridiagonal. Every iteration produces a new tridiagonal matrix which is by one row and one column bigger than the previous one. With growing size of the matrix its eigenvalues converge against the true ones until, in the case of finite dimensional Hilbert spaces, the eigenvalues reach their true values. The key point is that the extremal eigenvalues converge rather quickly compared to the other ones [60]. Thus it might be that after 300 Lanczos steps the ground state energy is already approximated to 10 figures although the dimension of the underlying Hilbert space is $10^8$.

A simple Lanczos algorithm looks like the following. One starts with an arbitrary vector $| \psi_0 \rangle$, which has to have an overlap with the (unknown) ground state. The next orthogonal vector is constructed by application of $\underset{\sim}{H}$ and projecting out the original vector $| \psi_0 \rangle$

$$| \psi_1' \rangle = (1 - | \psi_0 \rangle \langle \psi_0 |) \underset{\sim}{H} | \psi_0 \rangle = \underset{\sim}{H} | \psi_0 \rangle - \langle \psi_0 | \underset{\sim}{H} | \psi_0 \rangle | \psi_0 \rangle , \tag{29}$$

which yields the normalized vector

$$| \psi_1 \rangle = \frac{| \psi_1' \rangle}{\sqrt{\langle \psi_1' | \psi_1' \rangle}} . \tag{30}$$

Similarly all further basis vectors are generated

$$\begin{aligned} | \psi_{k+1}' \rangle &= (1 - | \psi_k \rangle \langle \psi_k | - | \psi_{k-1} \rangle \langle \psi_{k-1} |) \underset{\sim}{H} | \psi_k \rangle \\ &= \underset{\sim}{H} | \psi_k \rangle - \langle \psi_k | H | \psi_k \rangle | \psi_k \rangle - \langle \psi_{k-1} | \underset{\sim}{H} | \psi_k \rangle | \psi_{k-1} \rangle \end{aligned} \tag{31}$$

and

$$| \psi_{k+1} \rangle = \frac{| \psi_{k+1}' \rangle}{\sqrt{\langle \psi_{k+1}' | \psi_{k+1}' \rangle}} . \tag{32}$$

The new Lanczos vector is by construction orthogonal to the two previous ones. Without proof we repeat that it is then also orthogonal to all other previous Lanczos vectors. This constitutes the tridiagonal form of the resulting Hamilton matrix

$$T_{i,j} = \langle \psi_i | \underset{\sim}{H} | \psi_j \rangle \qquad \text{with} \qquad T_{i,j} = 0 \quad \text{if} \quad |i - j| > 1 . \tag{33}$$

The Lanczos matrix $T$ can be diagonalized at any step. Usually one iterates the method until a certain convergence criterion is fulfilled.

The eigenvectors of $\underset{\sim}{H}$ can be approximated using the eigenvectors $|\,\phi_\mu\,\rangle$ of $T$

$$|\,\chi_\mu\,\rangle \approx \sum_{i=0}^{n} \langle\,\psi_i\,|\,\phi_\mu\,\rangle\,|\,\psi_i\,\rangle \,, \tag{34}$$

where $\mu$ labels the desired energy eigenvalue, e. g. the ground state energy. $n$ denotes the number of iterations.

The simple Lanczos algorithm has some problems due to limited accuracy. One problem is that eigenvalues may collapse. Such problems can be solved with more refined formulations of the method [59].


**DMRG**

The DMRG technique [61] has become one of the standard numerical methods for quantum lattice calculations in recent years [62, 63]. Its basic idea is the reduction of Hilbert space while focusing on the accuracy of a target state. For this purpose the system is divided into subunits – blocks – which are represented by reduced sets of basis states. The dimension $m$ of the truncated block Hilbert space is a major input parameter of the method and to a large extent determines its accuracy.

DMRG is best suited for chain-like structures. Many accurate results have been achieved by applying DMRG to various (quasi-)one-dimensional systems [64, 56, 65]. The best results were found for the limit of infinite chains with open boundary conditions. It is commonly accepted that DMRG reaches maximum accuracy when it is applied to systems with a small number of interactions between the blocks, e. g. systems with only nearest-neighbor interaction [62].

It is not *a priori* clear how good results for finite systems like magnetic molecules are[4]. Such systems are usually not chain-like, so in order to carry out DMRG calculations a mapping onto a one-dimensional structure has to be performed [62]. Since the spin array consists of a countable number of spins, any arbitrary numbering is already a mapping onto a one-dimensional structure. However, even if the original system had only nearest-neighbor exchange, the new one-dimensional system has many long-range interactions depending on the way the spins are enumerated. Therefore, a numbering which minimizes long range interactions is preferable. Fig. 6 shows the graph of interactions for the molecule $\{Mo_{72}Fe_{30}\}$ which we want to consider as an example in the following [66].
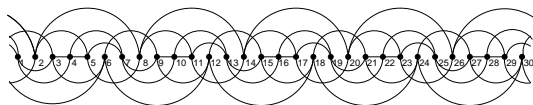


**Fig. 6:** *One-dimensional projection of the icosidodecahedron: the lines represent interactions.*

For finite systems a block algorithm including sweeps, which is similar to the setup in White's original article [61], has turned out to be most efficient. Two blocks are connected via two single spin sites, these four parts form the superblock see Fig. 7.

For illustrative purposes we use a simple Heisenberg Hamiltonian, compare (2). The Hamiltonian is invariant under rotations in spin space. Therefore, the total magnetic quantum number

---

[4]Work done with Matthias Exler, Universität Osnabrück, Germany.
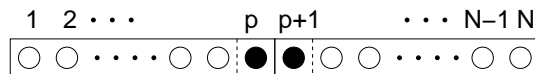
**Fig. 7:** *Block setup for DMRG "sweep" algorithm: The whole system of $N$ spins constitutes the superblock. The spins $\{1, 2, \ldots, p\}$ belong to the left block, the other spins $\{p+1, \ldots, N\}$ to the right block.*
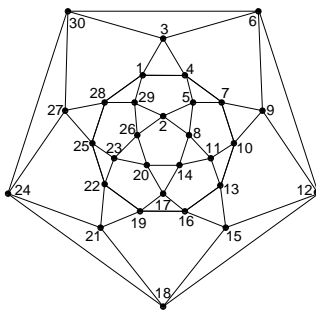


**Fig. 8:** *Two-dimensional projection of the icosidodecahedron, the site numbers are those used in our DMRG algorithm.*

$M$ is a good quantum number and we can perform our calculation in each orthogonal subspace $\mathcal{H}(M)$ separately.

Since it is difficult to predict the accuracy of a DMRG calculation, it is applied to an exactly diagonalizable system first. The most realistic test system for the use of DMRG for $\{Mo_{72}Fe_{30}\}$ is the icosidodecahedron with spins $s = 1/2$. This fictitious molecule, which possibly may be synthesized with vanadium ions instead of iron ions, has the same structure as $\{Mo_{72}Fe_{30}\}$, but the smaller spin quantum number reduces the dimension of the Hilbert space significantly. Therefore a numerically exact determination of low-lying levels using a Lanczos method is possible [67]. These results are used to analyze the principle feasibility and the accuracy of the method.

The DMRG calculations were implemented using the enumeration of the spin sites as shown in Figs. 6 and 8. This enumeration minimizes the average interaction length between two sites.

In Fig. 9 the DMRG results (crosses) are compared to the energy eigenvalues (circles) determined numerically with a Lanczos method [67, 66]. Very good agreement of both sequences, with a maximal relative error of less than 1% is found. Although the high accuracy of one-dimensional calculations (often with a relative error of the order of $10^{-6}$) is not achieved, the result demonstrates that DMRG is applicable to finite 2D spin systems. Unfortunately, increasing $m$ yields only a weak convergence of the relative error, which is defined relative to the width of the spectrum

$$\epsilon(m) = \frac{E_{\mathrm{DMRG}}(m) - E_0}{|E_0^{\mathrm{AF}} - E_0^{\mathrm{F}}|} \ . \tag{35}$$

The dependence for a quasi two-dimensional structure like the icosidodecahedron is approximately proportional to $1/m$ (see Fig. 10). Unfortunately, such weak convergence is characteristic for two-dimensional systems in contrast to one-dimensional chain structures, where the relative error of the approximate energy was reported to decay exponentially with $m$ [61]. Nevertheless, the extrapolated ground state energy for $s = 1/2$ deviates only by $\epsilon = 0.7$ % from the
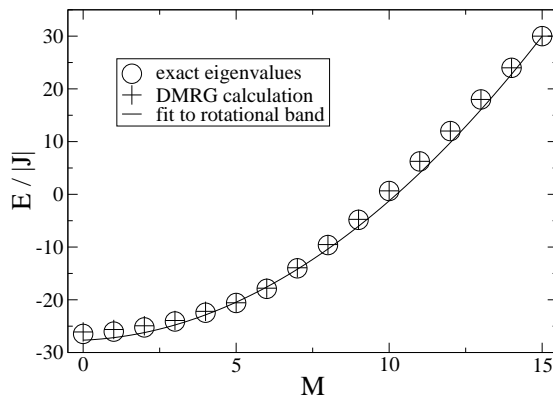
**Fig. 9:** *Minimal energy eigenvalues of the $s = 1/2$ icosidodecahedron. The DMRG result with $m = 60$ is depicted by crosses, the Lanczos values by circles. The rotational band is discussed in subsection 3.4.*

ground state energy determined with a Lanczos algorithm.
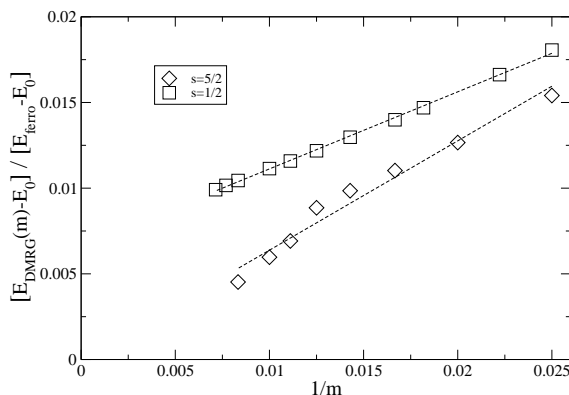


**Fig. 10:** *Dependence of the approximate ground state energy on the DMRG parameter $m$. $E_0$ is the true ground state energy in the case $s = 1/2$ and the extrapolated one for $s = 5/2$.*

The major result of the presented investigation is that the DMRG approach delivers acceptable results for finite systems like magnetic molecules. Nevertheless, the accuracy known from one-dimensional systems is not reached.

## Spin-coherent states

Spin-coherent states [68] provide another means to either treat a spin system exactly and investigate for instance its dynamics [69] or to use spin coherent states in order to approximate the low-lying part of the spectrum. They are also used in connection with path integral methods. In the following the basic ideas and formulae will be presented.

The obvious advantage of spin-coherent states is that they provide a bridge between classical spin dynamics and quantum spin dynamics. Spin coherent states are very intuitive since they parameterize a quantum state by the expectation value of the spin operator, e. g. by the two angles which represent the spin direction.

Spin coherent states $|z\rangle$ are defined as

$$|z\rangle = \frac{1}{(1+|z|^2)^s} \sum_{p=0}^{2s} \sqrt{\binom{2s}{p}} \, z^p \, |s, m = s - p\rangle \,, \quad z \in \mathbb{C} \,. \tag{36}$$

In this definition spin-coherent states are characterized by the spin length $s$ and a complex value $z$. The states (36) are normalized but not orthogonal

$$\langle z | z \rangle = 1 \,, \quad \langle y | z \rangle = \frac{(1 + y^* z)^{2s}}{(1 + |y|^2)^s (1 + |z|^2)^s} \,.$$

Spin-coherent states provide a basis in single-spin Hilbert space, but they form an overcomplete set of states. Their completeness relation reads

$$\underset{\sim}{\mathbb{1}} = \frac{2s+1}{\pi} \int d^2 z \frac{|z\rangle\langle z|}{(1+|z|^2)^2} \,, \quad d^2 z = d\mathrm{Re}(z) \, d\mathrm{Im}(z) \,. \tag{37}$$

The intuitive picture of spin-coherent states becomes obvious if one transforms the complex number $z$ into angles on a Riemann sphere

$$z = \tan(\theta/2) e^{i\phi} \,, \quad 0 \le \theta < \pi \,, \quad 0 \le \phi < 2\pi \,. \tag{38}$$

Thus, spin-coherent states may equally well be represented by two polar angles $\theta$ and $\phi$. Then the expectation value of the spin operator $\underset{\sim}{\vec{s}}$ is simply

$$\langle \theta, \phi | \underset{\sim}{\vec{s}} | \theta, \phi \rangle = s \begin{pmatrix} \sin(\theta)\cos(\phi) \\ \sin(\theta)\sin(\phi) \\ \cos(\theta) \end{pmatrix} \,. \tag{39}$$

Using (38) the definition of the states $|\theta, \phi\rangle$ which is equivalent to Eq. (36) is then given by

$$|\theta, \phi\rangle = \sum_{p=0}^{2s} \sqrt{\binom{2s}{p}} \left[\cos(\theta/2)\right]^{(2s-p)} \left[e^{i\phi}\sin(\theta/2)\right]^p |s, m = s - p\rangle \tag{40}$$

and the completeness relation simplifies to

$$\underset{\sim}{\mathbb{1}} = \frac{2s+1}{4\pi} \int d\Omega \, |\theta, \phi\rangle\langle \theta, \phi| \,. \tag{41}$$

Product states of spin-coherent states span the many-spin Hilbert space. A classical ground state can easily be translated into a many-body spin-coherent state. One may hope that this state together with other product states can provide a useful set of linearly independent states in order to approximate low-lying states of systems which are too big to handle otherwise. But it is too early to judge the quality of such approximations.

## 3.3  Evaluation of thermodynamic observables

For the sake of completeness we want to outline how basic observables can be evaluated both as function of temperature $T$ and magnetic field $B$. We will assume that $\left[\underset{\sim}{H}, \underset{\sim}{S_z}\right] = 0$ for this

part, so that the energy eigenvectors $| \nu \rangle$ can be chosen as simultaneous eigenvectors of $\underset{\sim}{S}_z$ with eigenvalues $E_\nu(B)$ and $M_\nu$. The energy dependence of $E_\nu(B)$ on $B$ is simply given by the Zeeman term. If $\underset{\sim}{H}$ and $\underset{\sim}{S}_z$ do not commute the respective traces for the partition function and thermodynamic means have to be evaluated starting from their general definitions.
The partition function is defined as follows

$$Z(T,B) \;=\; \mathrm{tr}\left\{\mathrm{e}^{-\beta \underset{\sim}{H}}\right\} = \sum_\nu \mathrm{e}^{-\beta E_\nu(B)} \,. \tag{42}$$

Then the magnetization and the susceptibility per molecule can be evaluated from the first and the second moment of $\underset{\sim}{S}_z$

$$\mathcal{M}(T,B) \;=\; -\frac{1}{Z}\,\mathrm{tr}\left\{g\mu_B \underset{\sim}{S}_z \mathrm{e}^{-\beta \underset{\sim}{H}}\right\} \tag{43}$$

$$=\; -\frac{g\mu_B}{Z}\sum_\nu M_\nu\,\mathrm{e}^{-\beta E_\nu(B)}$$

$$\chi(T,B) \;=\; \frac{\partial \mathcal{M}(T,B)}{\partial B} \tag{44}$$

$$=\; \frac{(g\mu_B)^2}{k_B T}\left\{\frac{1}{Z}\sum_\nu M_\nu^2\,\mathrm{e}^{-\beta E_\nu(B)} - \left(\frac{1}{Z}\sum_\nu M_\nu\,\mathrm{e}^{-\beta E_\nu(B)}\right)^2\right\}\,.$$

In a similar way the internal energy and the specific heat are evaluated from first and second moment of the Hamiltonian

$$U(T,B) \;=\; -\frac{1}{Z}\,\mathrm{tr}\left\{\underset{\sim}{H}\mathrm{e}^{-\beta \underset{\sim}{H}}\right\} \tag{45}$$

$$=\; -\frac{1}{Z}\sum_\nu E_\nu(B)\,\mathrm{e}^{-\beta E_\nu(B)}$$

$$C(T,B) \;=\; \frac{\partial U(T,B)}{\partial B} \tag{46}$$

$$=\; \frac{1}{k_B T^2}\left\{\frac{1}{Z}\sum_\nu (E_\nu(B))^2\,\mathrm{e}^{-\beta E_\nu(B)} - \left(\frac{1}{Z}\sum_\nu E_\nu(B)\,\mathrm{e}^{-\beta E_\nu(B)}\right)^2\right\}\,.$$

### 3.4   Properties of spectra

In the following chapter I am discussing some properties of the spectra of magnetic molecules with isotropic and antiferromagnetic interaction.

**Non-bipartite spin rings**

With the advent of magnetic molecules it appears to be possible to synthesize spin rings with an odd number of spins. Although related to infinite spin rings and chains such systems have not been considered mainly since it does not really matter whether an infinite ring has an odd or an even number of spins. In addition the sign rule of Marshall and Peierls [70] and the famous theorems of Lieb, Schultz, and Mattis [71, 72] provided valuable tools for the understanding of even rings which have the property to be bipartite and are thus non-frustrated. These theorems explain the degeneracy of the ground states in subspaces $\mathcal{H}(M)$ as well as their shift quantum number $k$ or equivalently crystal momentum quantum number $p_k = 2\pi k/N$.

| $s$ | $N$ | | | | | | | | | |
|---|---|---|---|---|---|---|---|---|---|---|
| | 2 | 3 | 4 | 5 | 6 | 7 | 8 | 9 | 10 | |
| $\frac{1}{2}$ | 1.5 | 0.5 | 1 | 0.747 | 0.934 | 0.816 | 0.913 | 0.844 | 0.903 | $E_0/(NJ)$ |
| | 1 | 4 | 1 | 4 | 1 | 4 | 1 | 4 | 1 | deg |
| | 0 | 1/2 | 0 | 1/2 | 0 | 1/2 | 0 | 1/2 | 0 | $S$ |
| | 1 | 1, 2 | 0 | 1, 4 | 3 | 2, 5 | 0 | 2, 7 | 5 | $k$ |
| $\frac{1}{2}$ | 4.0 | 3.0 | 2.0 | 2.236 | 1.369 | 2.098 | 1.045 | 1.722 | 0.846 | $\Delta E/|J|$ |
| | 3 | 4 | 3 | 2 | 3 | 8 | 3 | 8 | 3 | deg |
| | 1 | 3/2 | 1 | 1/2 | 1 | 3/2 | 1 | 3/2 | 1 | $S$ |
| | 0 | 0 | 2 | 0 | 0 | 1, 6 | 4 | 3, 6 | 0 | $k$ |
| 1 | 4 | 2 | 3 | 2.612 | 2.872 | 2.735 | 2.834 | 2.773 | 2.819 | $E_0/(NJ)$ |
| | 1 | 1 | 1 | 1 | 1 | 1 | 1 | 1 | 1 | deg |
| | 0 | 0 | 0 | 0 | 0 | 0 | 0 | 0 | 0 | $S$ |
| | 0 | 0 | 0 | 0 | 0 | 0 | 0 | 0 | 0 | $k$ |
| 1 | 4.0 | 2.0 | 2.0 | 1.929 | 1.441 | 1.714 | 1.187 | 1.540 | 1.050 | $\Delta E/|J|$ |
| | 3 | 9 | 3 | 6 | 3 | 6 | 3 | 6 | 3 | deg |
| | 1 | 1 | 1 | 1 | 1 | 1 | 1 | 1 | 1 | $S$ |
| | 1 | 0, 1, 2 | 2 | 2, 3 | 3 | 3, 4 | 4 | 4, 5 | 5 | $k$ |

**Table 1:** *Properties of ground and first excited state of AF Heisenberg rings for various $N$ and $s$: ground state energy $E_0$, gap $\Delta E$, degeneracy $\mathrm{deg}$, total spin $S$ and shift quantum number $k$.*

Nowadays exact diagonalization methods allow to evaluate eigenvalues and eigenvectors of $\underset{\sim}{H}$ for small even and odd spin rings of various numbers $N$ of spin sites and spin quantum numbers $s$ where the interaction is given by antiferromagnetic nearest neighbor exchange [52, 53, 54, 73, 74, 75]. Although Marshall-Peierls sign rule and the theorems of Lieb, Schultz, and Mattis do not apply to non-bipartite rings, i. e. frustrated rings with odd $N$, it turns out that such rings nevertheless show astonishing regularities[5]. Unifying the picture for even and odd $N$, we find for the ground state without exception [74, 75]:

1. The ground state belongs to the subspace $\mathcal{H}(S)$ with the smallest possible total spin quantum number $S$; this is either $S = 0$ for $N \cdot s$ integer, then the total magnetic quantum number $M$ is also zero, or $S = 1/2$ for $N \cdot s$ half integer, then $M = \pm 1/2$.

2. If $N \cdot s$ is integer, then the ground state is non-degenerate.

3. If $N \cdot s$ is half integer, then the ground state is fourfold degenerate.

4. If $s$ is integer or $N \cdot s$ even, then the shift quantum number is $k = 0$.

5. If $s$ is half integer and $N \cdot s$ odd, then the shift quantum number turns out to be $k = N/2$.

6. If $N \cdot s$ is half integer, then $k = \lfloor (N + 1)/4 \rfloor$ and $k = N - \lfloor (N + 1)/4 \rfloor$ is found. $\lfloor (N + 1)/4 \rfloor$ symbolizes the greatest integer less or equal to $(N + 1)/4$.

[5]Work done with Klaus Bärwinkel and Heinz-Jürgen Schmidt, Universität Osnabrück, Germany.

| $s$ | | | | | $N$ | | | | | |
|---|---|---|---|---|---|---|---|---|---|---|
| | 2 | 3 | 4 | 5 | 6 | 7 | 8 | 9 | 10 | |
| $\frac{3}{2}$ | 7.5 | 3.5 | 6 | 4.973 | 5.798 | 5.338 | 5.732 | 5.477 | 5.704[††] | $E_0/(NJ)$ |
| | 1 | 4 | 1 | 4 | 1 | 4 | 1 | 4 | 1 | deg |
| | 0 | 1/2 | 0 | 1/2 | 0 | 1/2 | 0 | 1/2 | 0 | $S$ |
| | 1 | 1, 2 | 0 | 1, 4 | 3 | 2, 5 | 0 | 2, 7 | 5 | $k$ |
| $\frac{3}{2}$ | 4.0 | 3.0 | 2.0 | 2.629 | 1.411 | 2.171 | 1.117 | 1.838 | 0.938[††] | $\Delta E/|J|$ |
| | 3 | 16 | 3 | 8 | 3 | 8 | 3 | 8 | 3 | deg |
| | 1 | 3/2 | 1 | 3/2 | 1 | 3/2 | 1 | 3/2 | 1 | $S$ |
| | 0 | 0, 1, 2 | 2 | 2, 3 | 0 | 1, 6 | 4 | 3, 6 | 0 | $k$ |
| 2 | 12 | 6 | 10 | 8.456 | 9.722 | 9.045 | 9.630 | 9.263[††] | 9.590[††] | $E_0/(NJ)$ |
| | 1 | 1 | 1 | 1 | 1 | 1 | 1 | 1 | 1 | deg |
| | 0 | 0 | 0 | 0 | 0 | 0 | 0 | 0 | 0 | $S$ |
| | 0 | 0 | 0 | 0 | 0 | 0 | 0 | 0 | 0 | $k$ |
| 2 | 4.0 | 2.0 | 2.0 | 1.922 | 1.394 | 1.652 | 1.091 | 1.431[††] | 0.906[††] | $\Delta E/|J|$ |
| | 3 | 9 | 3 | 6 | 3 | 6 | 3 | 6 | 3 | deg |
| | 1 | 1 | 1 | 1 | 1 | 1 | 1 | 1 | 1 | $S$ |
| | 1 | 0, 1, 2 | 2 | 2, 3 | 3 | 3, 4 | 4 | 4, 5 | 5 | $k$ |
| $\frac{5}{2}$ | 17.5 | 8.5 | 15 | 12.434 | 14.645 | 13.451 | 14.528[†] | 13.848[††] | 14.475[††] | $E_0/(NJ)$ |
| | 1 | 4 | 1 | 4 | 1 | 4 | 1 | 4 | 1 | deg |
| | 0 | 1/2 | 0 | 1/2 | 0 | 1/2 | 0 | 1/2 | 0 | $S$ |
| | 1 | 1, 2 | 0 | 1,4 | 3 | 2, 5 | 0 | 2, 7 | 5 | $k$ |

**Table 2:** *Properties of ground and first excited state of AF Heisenberg rings for various $N$ and $s$ (continuation): ground state energy $E_0$, gap $\Delta E$, degeneracy deg, total spin $S$ and shift quantum number $k$. † – O. Waldmann, private communication. †† – projection method [55].*

In the case of $s = 1/2$ one knows the $k$-quantum numbers for all $N$ via the Bethe ansatz [54, 73], and for spin $s = 1$ and even $N$ the $k$ quantum numbers are consistent with Ref. [53]. It appears that for the properties of the first excited state such rules do not hold in general, but only for "high enough" $N > 5$ [75]. Then, as can be anticipated from tables 1 and 2, we can conjecture that

- if $N$ is even, then the first excited state has $S = 1$ and is threefold degenerate, and

- if $N$ is odd and the single particle spin is half-integer, then the first excited state has $S = 3/2$ and is eightfold degenerate, whereas

- if $N$ is odd and the single particle spin is integer, then the first excited state has $S = 1$ and is sixfold degenerate.

Considering relative ground states in subspaces $\mathcal{H}(M)$ one also finds – for even as well as for odd $N$ – that the shift quantum numbers $k$ show a strikingly simple regularity for $N \neq 3$

$$k \equiv \pm(Ns - M)\lceil \frac{N}{2} \rceil \mod N , \qquad (47)$$

where $\lceil N/2 \rceil$ denotes the smallest integer greater than or equal to $N/2$ [76]. For $N = 3$ and $3s - 2 \geq |M| \geq 1$ one finds besides the ordinary $k$-quantum numbers given by (47) extraordinary $k$-quantum numbers, which supplement the ordinary ones to the complete set $\{k\} = \{0, 1, 2\}$.

For even $N$ the $k$ values form an alternating sequence $0, N/2, 0, N/2, \ldots$ on descending from the magnon vacuum with $M = Ns$ as known from the sign-rule of Marshall and Peierls [70]. For odd $N$ it happens that the ordinary $k$-numbers are repeated on descending from $M \leq Ns - 1$ to $M - 1$ iff $N$ divides $[2(Ns - M) + 1]$.

Using the $k$-rule one can as well derive a rule for the relative ground state energies and for the respective $S$ quantum numbers:

- For the relative ground state energies one finds that if the $k$-number is different in adjacent subspaces, $E_{\min}(S) < E_{\min}(S+1)$ holds. If the $k$-number is the same, the energies could as well be the same.

- Therefore, if $N$ (even or odd) does not divide $(2(Ns - M) + 1)\lceil N/2 \rceil$, then any relative ground state in $\mathcal{H}(M)$ has the total spin quantum number $S = |M|$.

- This is always true for the absolute ground state which therefore has $S = 0$ for $Ns$ integer and $S = 1/2$ for $Ns$ half integer.

The $k$-rule (47) is founded in a mathematically rigorous way for $N$ even [70, 71, 72], $N = 3$, $M = Ns$, $M = Ns - 1$, and $M = Ns - 2$ [76]. An asymptotic proof for large enough $N$ can be provided for systems with an asymptotically finite excitation gap, i. e. systems with integer spin $s$ for which the Haldane conjecture applies [77, 78]. In all other cases numerical evidence was collected and the $k$-rule as a conjecture still remains a challenge [76].

**Rotational bands**

For many spin systems with constant isotropic antiferromagnetic nearest neighbor Heisenberg exchange the minimal energies $E_{min}(S)$ form a rotational band, i. e. depend approximately quadratically on the total spin quantum number $S$ [79, 80, 81]

$$E_{min}(S) \approx E_a - J \frac{D(N, s)}{N} S(S + 1) . \tag{48}$$

The occurrence of a rotational band has been noted on several occasions for an even number of spins defining a ring structure, e. g. see Ref. [81]. The minimal energies have been described as "following the Landé interval rule" [28, 29, 30, 32]. However, we[6] find that the same property also occurs for rings with an odd number of spins as well as for the various polytope configurations we have investigated, in particular for quantum spins positioned on the vertices of a tetrahedron, cube, octahedron, icosahedron, triangular prism, and an axially truncated icosahedron. Rotational modes have also been found in the context of finite square and triangular lattices of spin-$1/2$ Heisenberg antiferromagnets [82, 83].

There are several systems, like spin dimers, trimers, squares, tetrahedra, and octahedra which possess a strict rotational band since their Hamiltonian can be simplified by quadrature. As an

---

[6]Work done together with Marshall Luban, Ames Lab, Iowa, USA.

example the Heisenberg square, i. e., a ring with $N = 4$ is presented. Because the Hamilton operator (23) can be rewritten as

$$\underset{\sim}{H} = -J \left( \underset{\sim}{\vec{S}^2} - \underset{\sim}{\vec{S}^2_{13}} - \underset{\sim}{\vec{S}^2_{24}} \right) , \tag{49}$$

$$\underset{\sim}{\vec{S}_{13}} = \underset{\sim}{\vec{s}}(1) + \underset{\sim}{\vec{s}}(3) , \ \underset{\sim}{\vec{S}_{24}} = \underset{\sim}{\vec{s}}(2) + \underset{\sim}{\vec{s}}(4) , \tag{50}$$

with all spin operators $\underset{\sim}{\vec{S}^2}$, $\underset{\sim}{\vec{S}^2_{13}}$ and $\underset{\sim}{\vec{S}^2_{24}}$ commuting with each other and with $\underset{\sim}{H}$, one can directly obtain the complete set of eigenenergies, and these are characterized by the quantum numbers $S$, $S_{13}$ and $S_{24}$. In particular, the lowest energy for a given total spin quantum number $S$ occurs for the choice $S_{13} = S_{24} = 2s$

$$E_{min}(S) = -J \left[ S \left( S + 1 \right) - 2 \cdot 2s \left( 2s + 1 \right) \right] = E_0 - J S \left( S + 1 \right) , \tag{51}$$

where $E_0 = 4s(2s + 1)J$ is the exact ground state energy. The various energies $E_{min}(S)$ form a rigorous parabolic rotational band of excitation energies. Therefore, these energies coincide with a parabolic fit (crosses connected by the dashed line on the l.h.s. of Fig. 11) passing through the antiferromagnetic ground state energy and the highest energy level, i. e., the ground state energy of the corresponding ferromagnetically coupled system.
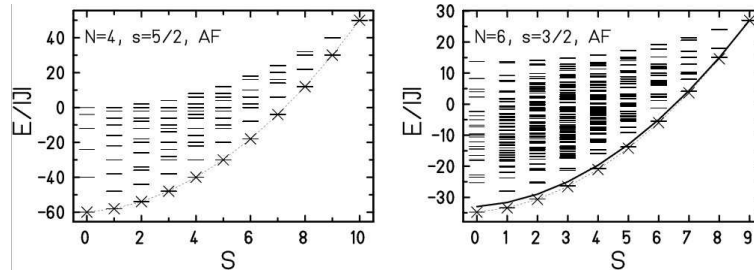


**Fig. 11:** *Energy spectra of antiferromagnetically coupled Heisenberg spin rings (horizontal dashes). The crosses connected by the dashed line represent the fit to the rotational band according to (51), which matches both the lowest and the highest energies exactly. On the l.h.s the dashed line reproduces the exact rotational band, whereas on the r.h.s. it only approximates it, but to high accuracy. The solid line on the r.h.s. corresponds to the approximation Eq. (52).*

It turns out that an accurate formula for the coefficient $D(N, s)$ of (51) can be developed using the sublattice structure of the spin array [79]. As an example we repeat the basic ideas for Heisenberg rings with an even number of spin sites [32]. Such rings are bipartite and can be decomposed into two sublattices, labeled $A$ and $B$, with every second spin belonging to the same sublattice. The classical ground state (Néel state) is given by an alternating sequence of opposite spin directions. On each sublattice the spins are mutually parallel. Therefore, a quantum trial state, where the individual spins on each sublattice are coupled to their maximum values, $S_A = S_B = Ns/2$, could be expected to provide a reasonable approximation to the true ground state, especially if $s$ assumes large values. For rings with even $N$ the approximation to the respective minimal energies for each value of the total spin $\underset{\sim}{\vec{S}} = \underset{\sim}{\vec{S}_A} + \underset{\sim}{\vec{S}_B}$ is then given by [32]

$$E^{approx}_{min}(S) = -\frac{4 J}{N} \left[ S(S + 1) - 2\frac{Ns}{2} \left( \frac{Ns}{2} + 1 \right) \right] . \tag{52}$$

This approximation exactly reproduces the energy of the highest energy eigenvalue, i. e., the ground state energy of the corresponding ferromagnetically coupled system ($S = Ns$). For all smaller $S$ the approximate minimal energy $E_{min}^{approx}(S)$ is bounded from below by the true one (Rayleigh-Ritz variational principle). The solid curve displays this behavior for the example of $N = 6$, $s = 3/2$ in Fig. 11 (r.h.s.). The coefficient "4" in Eq. (52) is the classical value, i. e. for each fixed even $N$ the coefficient $D(N, s)$ approaches 4 with increasing $s$ [79].

The approximate spectrum, (52), is similar to that of two spins, $\vec{S}_A$ and $\vec{S}_B$, each of spin quantum number $Ns/2$, that are coupled by an effective interaction of strength $4J/N$. Therefore, one can equally well say, that the approximate rotational band considered in (52) is associated with an effective Hamilton operator

$$H^{approx} = -\frac{4J}{N}\left[\vec{S}^2 - \vec{S}_A^2 - \vec{S}_B^2\right] , \tag{53}$$

where the two sublattice spins, $\vec{S}_A, \vec{S}_B$, assume their maximal value $S_A = S_B = Ns/2$. Hamiltonian (53) is also known as Hamiltonian of the Lieb-Mattis model which describes a system where each spin of one sublattice interacts with every spin of the other sublattice with equal strength [72, 84].
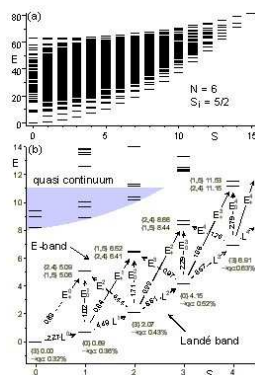


**Fig. 12:** *The low-lying levels of a spin ring, $N = 6$ and $s = 5/2$ in this example, can be grouped into the lowest (**L**andé) band, the first excited (**E**xcitation) band and the quasi-continuum (**QC**). For the spin levels of the L- and E-band $k$ is given in brackets followed by the energy. Arrows indicate strong transitions from the L-band. Associated numbers give the total oscillator strength $f_0$ for these transitions. With friendly permission by Oliver Waldmann [81].*

It is worth noting that this Hamiltonian reproduces more than the lowest levels in each subspace $\mathcal{H}(S)$. At least for bipartite systems also a second band is accurately reproduced as well as the gap to the quasi-continuum above, compare Figure 12 and Ref. [81]. This property is very useful since the approximate Hamiltonian allows the computation of several observables without diagonalizing the full Hamiltonian.

It is of course of utmost importance whether the band structure given by the approximate Hamiltonian (53) persists in the case of frustrated molecules. It seems that at least the minimal energies still form a rotational band which is understandable at least for larger spin quantum numbers $s$ taking into account that the parabolic dependence of the minimal energies on $S$ mainly reflects the classical limit for a wide class of spin systems [85].

The following example demonstrates that even in the case of the highly frustrated molecule $\{Mo_{72}Fe_{30}\}$ the minimal energies arrange as a "rotational band"[7]. In the case of $\{Mo_{72}Fe_{30}\}$

[7]Work done with Matthias Exler, Universität Osnabrück, Germany.

the spin system is decomposable into three sub-lattices with sub-lattice spin quantum numbers $S_A$, $S_B$, and $S_C$ [79, 80]. The corresponding approximate Hamilton operator reads

$$\underset{\sim}{H}_{\text{approx}} = -J\frac{D}{N}\left[\underset{\sim}{\vec{S}^2} - \gamma\left(\underset{\sim}{\vec{S}^2_A} + \underset{\sim}{\vec{S}^2_B} + \underset{\sim}{\vec{S}^2_C}\right)\right]\;, \tag{54}$$

where $\underset{\sim}{\vec{S}}$ is the total spin operator and the others are sub-lattice spin operators. $D$ and $\gamma$ are allowed to deviate from their respective classical values, $D = 6$ and $\gamma = 1$, in order to correct for finite $s$.
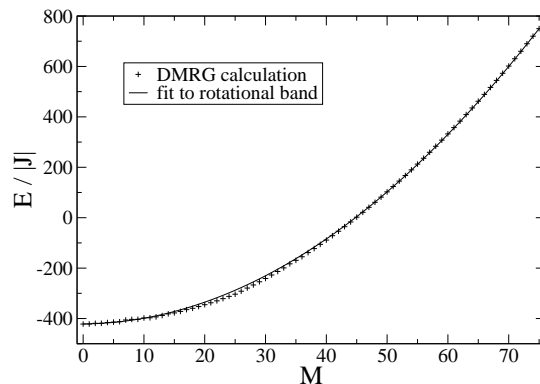


**Fig. 13:** *DMRG eigenvalues and lowest rotational band of the $s = 5/2$ icosidodecahedron; $m = 60$ was used except for the lowest and first exited level which were calculated with $m = 120$.*

We use the DMRG method to approximate the lowest energy eigenvalues of the full Hamiltonian and compare them to those predicted by the rotational band hypothesis (54). Fig. 13 shows the results and a fit to the lowest rotational band. Assuming the same dependence on $m$ as in the $s = 1/2$ case, the relative error of the DMRG data should also be less than $1\%$. The agreement between the DMRG energy levels and the predicted quadratic dependence is very good. Nevertheless, it remains an open question whether higher lying bands are present in such a highly frustrated compound.

**Magnetization jumps**
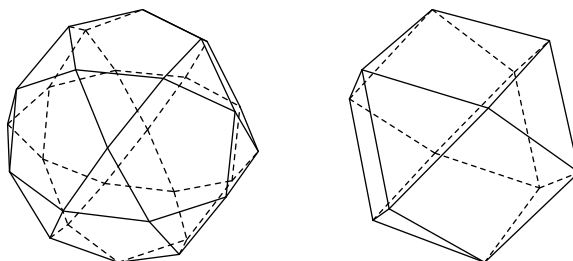


**Fig. 14:** *Structure of the icosidodecahedron (l.h.s.) and the cuboctahedron (r.h.s.).*

Although the spectra of many magnetic molecules possess a rotational band of minimal energies $E_{min}(S)$ and although in the classical limit, where the single-spin quantum number $s$ goes to infinity, the function $E_{min}(S)$ is even an exact parabola if the system has co-planar ground

states [85], we[8] find that for certain coupling topologies, including the cuboctahedron and the icosidodecahedron (see Fig. 14), that this rule is violated for high total spins [67, 86]. More precisely, for the icosidodecahedron the last four points of the graph of $E_{min}$ versus $S$, i. e. the points with $S = S_{max}$ to $S = S_{max} - 3$, lie on a straight line

$$E_{min}(S) = 60Js^2 - 6Js(30s - S) .$$ (55)

An analogous statement holds for the last three points of the corresponding graph for the cuboctahedron. These findings are based on numerical calculations of the minimal energies for several $s$ both for the icosidodecahedron as well as for the cuboctahedron. For both and other systems a rigorous proof of the high spin anomaly can be given [67, 87].

The idea of the proof can be summarized as follows: A necessary condition for the anomaly is certainly that the minimal energy in the one-magnon space is degenerate. Therefore, localized one-magnon states can be constructed which are also of minimal energy. When placing a second localized magnon on the spin array there will be a chance that it does not interact with the first one if a large enough separation can be achieved. This new two-magnon state is likely the state of minimal energy in the two-magnon Hilbert space because for antiferromagnetic interaction two-magnon bound states do not exist. This procedure can be continued until no further independent magnon can be placed on the spin array. In a sense the system behaves as if it consists of non-interacting bosons which, up to a limiting number, can condense into a single-particle ground state. In more mathematical terms: In order to prove the high-spin anomaly one first shows an inequality which says that all points $(S, E_{min}(S))$ lie above or on the line connecting the last two points. For specific systems as those mentioned above what remains to be done is to construct particular states which exactly assume the values of $E_{min}$ corresponding to the points lying on the bounding line, then these states are automatically states of minimal energy.
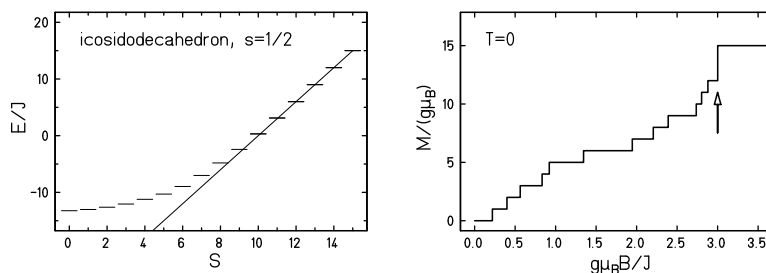


**Fig. 15:** *Icosidodecahedron: L.h.s. – minimal energy levels $E_{min}(S)$ as a function of total spin $S$. R.h.s. – magnetization curve at $T = 0$ [67].*

The observed anomaly – linear instead of parabolic dependence – results in a corresponding jump of the magnetization curve $\mathcal{M}$ versus $B$, see Fig. 15. In contrast, for systems which obey the Landé interval rule the magnetization curve at very low temperatures is a staircase with equal steps up to the highest magnetization. The anomaly could indeed be observed in magnetization measurements of the Keplerate molecules $\{Mo_{72}Fe_{30}\}$. Unfortunately, the magnetization measurements [36, 80] performed so far suffer from too high temperatures which smear out the anomaly.

---

[8]Work done with Heinz-Jürgen Schmidt, Universität Osnabrück, Andreas Honecker, Universität Braunschweig, Johannes Richter and Jörg Schulenburg, Universität Magdeburg, Germany.

Nevertheless, it may be possible to observe truly giant magnetization jumps in certain two-dimensional spin systems which possess a suitable coupling (e. g. Kagomé) [86]. In such systems the magnetization jump can be of the same order as the number of spins, i. e. the jump remains finite – or in other words is macroscopic – in the thermodynamic limit $N \to \infty$. Thus, this effect is a true macroscopic quantum effect.

# 4 Dynamics

In this section I would like to outline two branches – tunneling and relaxation – where the dynamics of magnetic molecules is investigated. The section is kept rather introductory since the field is rapidly evolving and it is too early to draw a final picture on all the details of the involved processes.

## 4.1 Tunneling

Tunneling dynamics has been one of the corner stones in molecular magnetism since its very early days, see e. g. [88, 21, 24, 89, 90].
The subject can roughly be divided into two parts, one deals with tunneling processes of the magnetization in molecules possessing a high ground state spin and an anisotropy barrier, the second deals with the remaining tunneling processes, e. g. in molecules which have an $S = 0$ ground state.
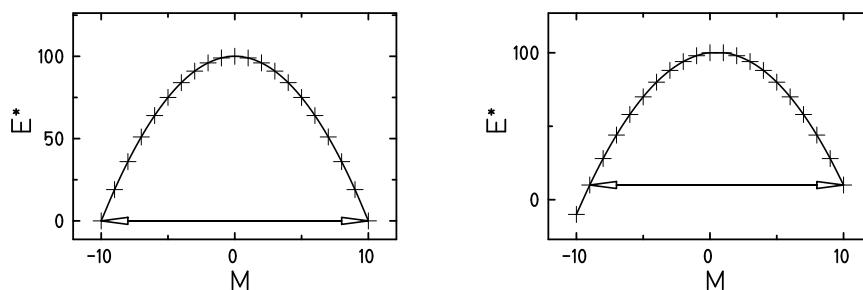


**Fig. 16:** *Sketch of the tunneling barrier for a high spin molecule with $S = 10$, l.h.s. without magnetic field, r.h.s. with magnetic field, compare Eq. (5). The arrows indicate a possible resonant tunneling process.*

As already mentioned in section 3.1 some molecules like $Mn_{12}$ and $Fe_8$ possess a high ground state spin. Since the higher lying levels are well separated from the low-lying $S = 10$ levels a single-spin Hamiltonian (5), which includes an anisotropy term, is appropriate. Figure 16 sketches the energy landscape for an anisotropy term which is quadratic in $\underset{\sim}{S}_z$. If the Hamiltonian includes terms like a magnetic field in $x$-direction that do not commute with $\underset{\sim}{S}_z$ resonant tunneling is observed between states $|\, S, M \,\rangle$ and $|\, S, -M \,\rangle$. This behavior is depicted on the l.h.s. of Fig. 16 for the transition between $M = -10$ and $M = 10$. If an additional magnetic field is applied in $z$-direction the quadratic barrier acquires an additional linear Zeeman term and is changed like depicted on the r.h.s. of Fig. 16. Now tunneling is possible between states of different $|M|$, see e. g. [91].
It is rather simple to model the tunneling process in the model Hilbert space of $S = 10$. i. e. a space with dimension $2S + 1 = 21$. Nevertheless, in a real substance the tunneling process

is accompanied and modified by other influences. The first major factor is temperature which may enhance the process, this leads to thermally assisted tunneling [92]. Each such substance hosts phonons which modify the tunneling process, too, resulting in phonon assisted tunneling [93, 94, 95, 96]. Then local dipolar fields and nuclear hyperfine fields may strongly affect the relaxation in the tunneling regime [6]. In addition there may be topological quenching due to the symmetry of the material [97, 98, 99]. And last but not least describing such complicated molecules not in effective single-spin models but in many-spin models is still in an unsatisfactory state, compare [100].
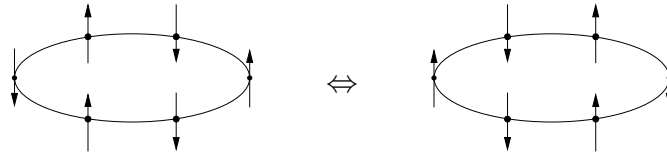


**Fig. 17:** *Sketch of the tunneling process between Néel-like states on a spin ring. Without loss of generality the state on the l.h.s. will be denoted by $|\,\text{Néel}, 1\,\rangle$ and the state on the r.h.s. will be denoted by $|\,\text{Néel}, 2\,\rangle$.*

Another kind of tunneling is considered for Heisenberg spin rings with uniaxial single-ion anisotropy. Classically the ground state of even rings like Na:Fe$_6$ and Cs:Fe$_8$ is given by a sequence of spin up and down like in Fig. 17. It now turns out that such a Néel-like state, which is formulated in terms of spin-coherent states (40), contributes dominantly to the true ground state as well as to the first excited state if the anisotropy is large enough [69]. Thus it is found that the ground state $|\,E_0\,\rangle$ and the first excited state $|\,E_1\,\rangle$ can be approximated as

$$
\begin{aligned}
|\,E_0\,\rangle &\approx \frac{1}{\sqrt{2}}\left(|\,\text{Néel}, 1\,\rangle \pm |\,\text{Néel}, 2\,\rangle\right) \\
|\,E_1\,\rangle &\approx \frac{1}{\sqrt{2}}\left(|\,\text{Néel}, 1\,\rangle \mp |\,\text{Néel}, 2\,\rangle\right),
\end{aligned}
\tag{56}
$$

where the upper sign is appropriate for rings where the number of spins $N$ is a multiple of 4, e. g. $N = 8$, and the lower sign is for all other even $N$.

Therefore, the tunneling frequency is approximately given by the gap between ground and first excited state. Experimentally, such a tunnel process is hard to observe, especially since ESR is sensitive only to the total spin. What would be needed is a local probe like NMR. This could be accomplished by replacing one of the iron ions by another isotope.

The tunneling process was further analyzed for various values of the uniaxial single-ion anisotropy [101]. Since in such a case the cyclic shift symmetry persists, $k$ is still a good quantum number. Therefore, mixing of states is only allowed between states with the same $k$ quantum number. This leads to the conclusion that the low-temperature tunneling phenomena can be understood as the tunneling of the spin vector between different rotational modes with $\Delta S = 2$, compare Fig. 18 and the subsection on rotational bands on page 19.

## 4.2 Relaxation dynamics

In a time-dependent magnetic field the magnetization tries to follow the field. Looking at this process from a microscopic point of view, one realizes that, if the Hamiltonian would commute with the Zeeman term, no transitions would occur, and the magnetization would not change a
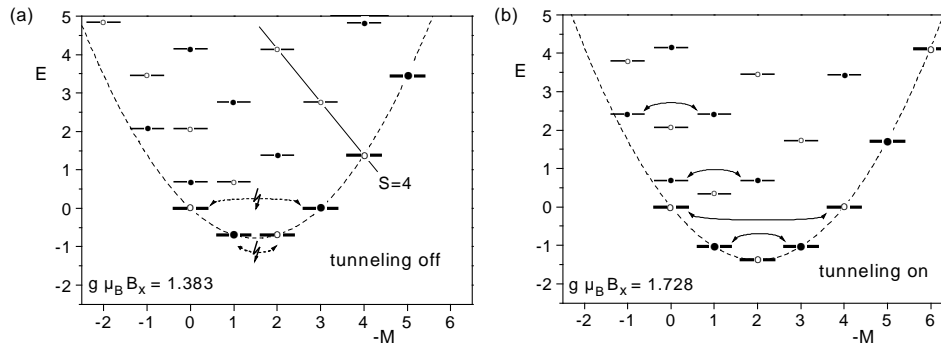
**Fig. 18:** *Energy spectrum of spin rings with $N = 6$ and vanishing anisotropy at two magnetic fields drawn as a function of the magnetic quantum number $M$. The dashed curves represent the lowest-lying parabolas $E_{min}(M)$ discussed in section 3.4. A white or black circle indicates that a state belongs to $k = 0$ or $k = N/2$, compare Fig. 12. States belonging to one spin multiplet are located on straight lines like that plotted in panel (a) for the $S = 4$ multiplet. With friendly permissions by Oliver Waldmann [101].*

tiny bit. There are basically two sources which permit transitions: non-commuting parts in the spin Hamiltonian and interactions with the surrounding. In the latter case the interaction with phonons seems to be most important.

Since a complete diagonalization of the full Hamiltonian including non-commuting terms as well as interactions like the spin-phonon interaction is practically impossible, both phenomena are modeled with the help of rate equations.
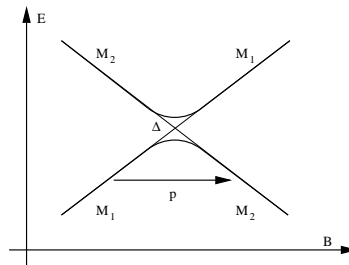


**Fig. 19:** *Schematic energy spectrum in the vicinity of an avoided level crossing. The formula by Landau, Zener, and Stückelberg (57) approximates the probability $p$ for the tunneling process from $M_1$ to $M_2$.*

If we start with a Hamiltonian $\underset{\sim}{H}_0$, which may be the Heisenberg Hamiltonian and add a non-commuting term $\underset{\sim}{H}'$ like anisotropy the eigenstates of the full Hamiltonian are superpositions of those of $\underset{\sim}{H}_0$. This expresses itself in avoided level crossings where the spectrum of $\underset{\sim}{H}_0$ would show level crossings, compare Fig. 19. Transitions between eigenstates of $\underset{\sim}{H}_0$, which may have good $M$ quantum numbers, can then effectively be modeled with the formula by Landau, Zener, and Stückelberg [102, 103, 104, 105, 106]

$$p \;=\; 1 - \exp\left\{ -\frac{\pi \Delta^2}{2\hbar g \mu_B |M_1 - M_2| \frac{d}{dt} B} \right\} . \tag{57}$$

$\Delta$ denotes the energy gap at the avoided level crossing.

The effect of phonons is taken into account by means of two principles: detailed balance, which models the desire of the system to reach thermal equilibrium and energy conservation, which takes into account that the energy released or absorbed by the spin system must be absorbed or released by the phonon system and finally exchanged with the thermostat. The interesting effects arise since the number of phonons is very limited at temperatures in the Kelvin-range or below, thus they may easily be used up after a short time (phonon bottleneck) and have to be provided by the thermostat around which needs a characteristic relaxation time. Since this all happens in a time-dependent magnetic field, the Zeeman splittings change all the time and phonons of different frequency are involved at each time step. In addition the temperature of the spin system changes during the process because the equilibration with the thermostat (liq. Helium) is not instantaneous. More accurately the process is not in equilibrium at all, especially for multi-level spin systems. Only for two-level systems the time-dependent occupation can be translated into an apparent temperature. In essence the retarded dynamics leads to distinct hysteresis loops which have the shape of a butterfly [107, 108, 109]. For more detailed information on dissipative two-level systems the interested reader is referred to Ref. [110, 109].

# 5  Magnetocalorics

The mean (internal) energy, the magnetization and the magnetic field are thermodynamic observables just as pressure and volume. Therefore, we can design thermodynamic processes which work with magnetic materials as a medium. This has of course already been done for a long time. The most prominent application is magnetization cooling which is mainly used to reach sub-Kelvin temperatures [111]. The first observation of sub-Kelvin temperatures is a nice example of how short an article can be to win the Nobel prize (Giauque, Chemistry, 1949). Meanwhile magnetization cooling is used in ordinary refrigerators.

768                        LETTERS  TO  THE  EDITOR

**Attainment of Temperatures Below 1° Absolute by Demagnetization of Gd₂(SO₄)₃·8H₂O**

We have recently carried out some preliminary experiments on the adiabatic demagnetization of $Gd_2(SO_4)_3$·$8H_2O$ at the temperatures of liquid helium. As previously predicted by one of us, a large fractional lowering of the absolute temperature was obtained.

An iron-free solenoid producing a field of about 8000 gauss was used for all the measurements. The amount of $Gd_2(SO_4)_3$·$8H_2O$ was 61 g. The observations were checked by many repetitions of the cooling. The temperatures were measured by means of the inductance of a coil surrounding the gadolinium sulfate. The coil was immersed in liquid helium and isolated from the gadolinium by means of an evacuated space. The thermometer was in excellent agreement with the temperature of liquid helium as indicated by its vapor pressure down to 1.5°K.

On March 19, starting at a temperature of about 3.4°K, the material cooled to 0.53°K. On April 8, starting at about 2°, a temperature of 0.34°K was reached. On April 9, starting at about 1.5°, a temperature of 0.25°K was attained.

It is apparent that it will be possible to obtain much lower temperatures, especially when successive demagnetizations are utilized.

W. F. GIAUQUE
D. P. MACDOUGALL

Department of Chemistry,
University of California,
Berkeley, California,
April 12, 1933.

**Fig. 20:** *The first observation of sub-Kelvin temperatures [111] is a nice example of how short an article can be to win the Nobel prize (Giauque, Chemistry, 1949).*

In early magnetocaloric experiments simple refrigerants like paramagnetic salts have been used. We will therefore consider such examples first.

For a paramagnet the Hamiltonian consists of the Zeeman term only. We then obtain for the

partition function

$$Z(T, B, N) = \left\{ \frac{\sinh[\beta g \mu_B B (s + 1/2)]}{\sinh[\beta g \mu_B B / 2]} \right\}^N . \tag{58}$$

Then the magnetization is

$$\mathcal{M}(T, B, N) = N g \mu_B \left\{ (s + 1/2) \coth[\beta g \mu_B B (s + 1/2)] - 1/2 \sinh[\beta g \mu_B B / 2] \right\} , \tag{59}$$

and the entropy reads

$$S(T, B, N) = N k_B \ln \left\{ \frac{\sinh[\beta g \mu_B B (s + 1/2)]}{\sinh[\beta g \mu_B B / 2]} \right\} - k_B \beta B \mathcal{M}(T, B, N) . \tag{60}$$

Besides their statistical definition both quantities follow from the general thermodynamic relationship

$$dF = \left( \frac{\partial F}{\partial T} \right)_B dT + \left( \frac{\partial F}{\partial B} \right)_T dB = -S dT - \mathcal{M} dB , \tag{61}$$

where $F(T, B, N) = -k_B T \ln[Z(T, B, N)]$.

Looking at Eq. (58) it is obvious that all thermodynamic observables for a paramagnet depend on temperature and field via the combination $B/T$, and so does the entropy. Therefore, an adiabatic demagnetization ($S = const$) means that the ratio $B/T$ has to remain constant, and thus temperature shrinks linearly with field, i.e.

$$\left( \frac{\partial T}{\partial B} \right)_S^{\text{para}} = \frac{T}{B} . \tag{62}$$

This situation changes completely for an interacting spin system. Depending on the interactions the adiabatic cooling rate $\frac{\partial T}{\partial B}$ can be smaller or bigger than the paramagnetic one (62) and even change sign, i.e. one would observe heating during demagnetization. It is nowadays understood that the cooling rate acquires extreme values close to phase transitions due to the excess entropy associated with such processes [112, 113, 114, 115].
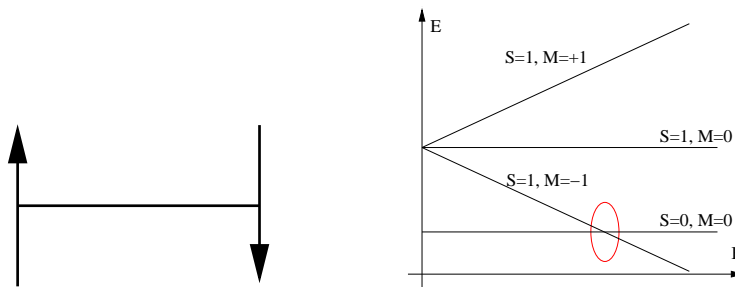


**Fig. 21:** *L.h.s.: Sketch of an antiferromagnetically coupled spin dimer. R.h.s.: Dependence of the energy levels on magnetic field for an antiferromagnetically coupled spin-$1/2$ dimer. At the critical field $B_c$ the lowest triplet level crosses the ground state level with $S = 0$.*

In the following this statement will be made clear by discussing the example of a simple anti-ferromagnetically coupled spin-$1/2$ dimer (Fig. 21, l.h.s.). In a magnetic field such a system
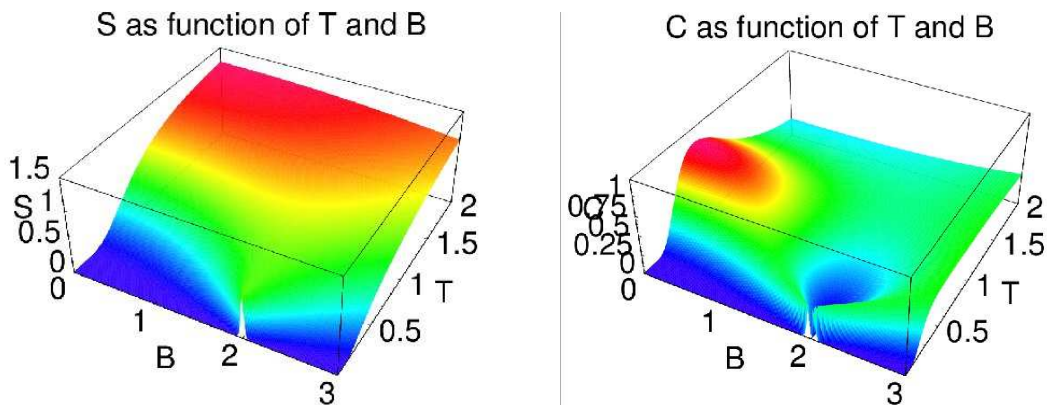
**Fig. 22:** *L.h.s.: Entropy of the dimer (Fig. 21) as function of $B$ and $T$. R.h.s.: Heat capacity of the dimer as function of $B$ and $T$.*

experiences a "quantum phase transition" if the lowest triplet level crosses the original ground state with $S = 0$, see Fig. 21, r.h.s.. Although one would hesitate to call such an ordinary ground state level crossing quantum phase transition it nevertheless is one. At $T = 0$ the magnetization $\mathcal{M}(T = 0, B)$ is a non-analytic function of the magnetic field $B$. At the critical field $B_c$ where the levels cross the magnetization exhibits a step.

In addition the entropy, which at $T = 0$ is zero for the non-degenerate ground state acquires a finite value at the critical field $B_c$ due to the degeneracy of the crossing levels. This enhancement remains present even at temperatures $T > 0$, compare Fig. 22, l.h.s.. In addition the heat capacity varies strongly around the critical field as is shown in Fig. 22, r.h.s..
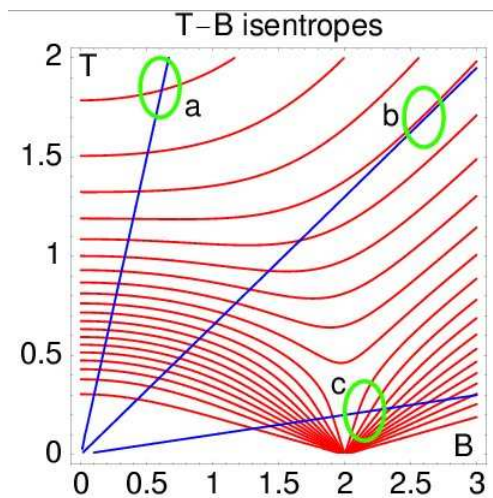


**Fig. 23:** *Isentrops of the spin dimer. The straight lines show the behavior of a paramagnet for comparison. $B$ is along the $x$-axis, $T$ along the $y$-axis.*

The behavior of the entropy as well as of the heat capacity explains how the adiabatic cooling rate

$$\left(\frac{\partial T}{\partial B}\right)_S = -T\frac{\left(\frac{\partial S}{\partial B}\right)_T}{C} \tag{63}$$

depends on field and temperature. Figure 23 shows the isentropes of the antiferromagnetically

coupled dimer both as function of field $B$ and temperature $T$. The straight lines show the behavior of a paramagnet for comparison. Three regions are highlighted.

- a: For low fields and high temperatures $\frac{\partial T}{\partial B}$ is smaller than for the paramagnet.

- b: For high fields and high temperatures the interacting system assumes the paramagnetic limit, i.e. $\frac{\partial T}{\partial B}$ is the same in both systems.

- c: For low temperatures and fields just above the critical field $\frac{\partial T}{\partial B}$ is much bigger than the cooling rate of the paramagnet.

- Not highlighted but nevertheless very exciting is the region at low temperature just below the critical field where the "cooling" rate $\frac{\partial T}{\partial B}$ has the opposite sign, i.e. upon demagnetizing the system heats up and upon magnetizing the system cools down.

The rate $\frac{\partial T}{\partial B}$ (63) depends directly on the derivative of the entropy with respect to the magnetic field. Therefore, it is clear that the effect will be enhanced if a high degeneracy can be obtained at some critical field. This is indeed possible in several frustrated materials where giant magnetization jumps to saturation are observed [86, 116, 114, 115].
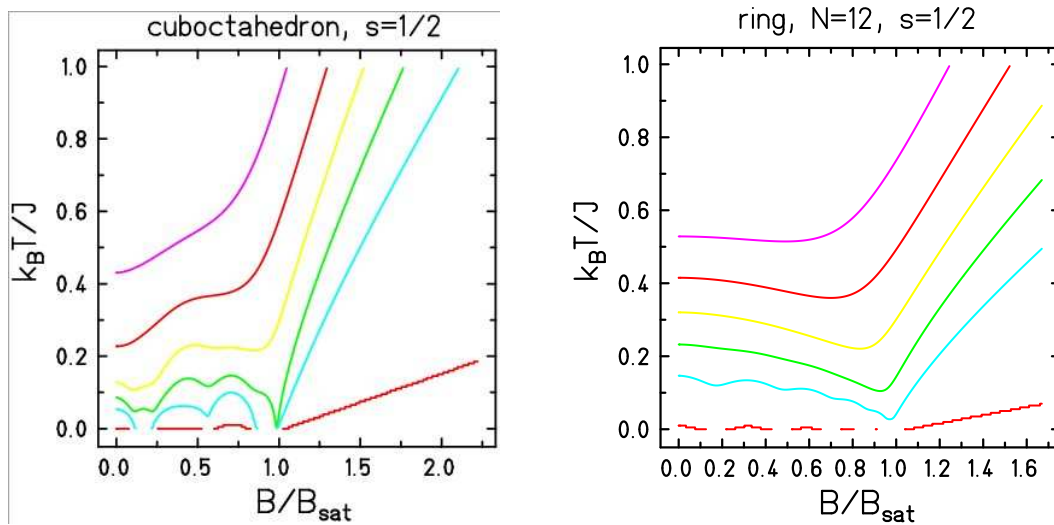


**Fig. 24:** *Isentropes of an antiferromagnetically coupled spin-$1/2$ cuboctahedron (l.h.s.) in comparison to the isentropes of an antiferromagnetically coupled spin ring of 12 spins with $s = 1/2$ (r.h.s.). The structure of the cuboctahedron is shown in Fig. 14 (r.h.s.).*

The following Figure 24 compares isentropes of an antiferromagnetically coupled spin-$1/2$ cuboctahedron (l.h.s.) with the isentropes of an antiferromagnetically coupled spin ring of 12 spins with $s = 1/2$ (r.h.s.). It is clearly visible that the cuboctahedral spin system has steeper isentropes than the ring system, and the reason is that the cuboctahedron features a larger jump to magnetization saturation ($\Delta M = 2$) than the spin ring ($\Delta M = 1$) which is connected with an enhanced degeneracy and thus higher entropy.

Summarizing, one can say that low-dimensional frustrated spin systems and especially magnetic molecules are substances with an interesting magnetocaloric behavior and may turn out to be useful new refrigerants for special applications.

**Acknowledgement**

# References

[1] R. Sessoli, D. Gatteschi, A. Caneschi, and M. A. Novak, Nature **365**, 141 (1993).

[2] D. Gatteschi, A. Caneschi, L. Pardi, and R. Sessoli, Science **265**, 1054 (1994).

[3] D. Gatteschi, Adv. Mater. **6**, 635 (1994).

[4] E. Coronado, P. Delhaes, D. Gatteschi, and J. Miller, eds., *Localized and Itinerant Molecular Magnetism: From Molecular Assemblies to the Devices*, vol. 321 of *NATO Advanced Studies Institute, Series E: Applied Sciences* (Kluwer Academic, Dordrecht, 1996).

[5] A. Müller, F. Peters, M. Pope, and D. Gatteschi, Chem. Rev. **98**, 239 (1998).

[6] A. Caneschi, D. Gatteschi, C. Sangregorio, R. Sessoli, L. Sorace, A. Cornia, M. A. Novak, C. Paulsen, and W. Wernsdorfer, J. Magn. Magn. Mater. **200**, 182 (1999).

[7] A. Müller, S. Sarkar, S. Q. N. Shah, H. Bögge, M. Schmidtmann, S. Sarkar, P. Kögerler, B. Hauptfleisch, A. Trautwein, and V. Schünemann, Angew. Chem., Int. Ed. **38**, 3238 (1999).

[8] M. N. Leuenberger and D. Loss, Nature **410**, 789 (2001).

[9] X. Wang and P. Zanardi, Phys. Lett. A **301**, 1 (2002).

[10] X. Wang, Phys. Rev. A **66**, 034302 (2002).

[11] P. Gütlich, A. Hauser, and H. Spiering, Angew. Chem. **106**, 2109 (1994).

[12] A. Bencini and D. Gatteschi, *Electron parametric resonance of exchange coupled systems* (Springer, Berlin, Heidelberg, 1990).

[13] C. Delfs, D. Gatteschi, L. Pardi, R. Sessoli, K. Wieghardt, and D. Hanke, Inorg. Chem. **32**, 3099 (1993).

[14] A. Caneschi, A. Cornia, A. C. Fabretti, D. Gatteschi, and W. Malavasi, Inorg. Chem. **34**, 4660 (1995).

[15] B. Pilawa, R. Desquiotz, M. Kelemen, M. Weickenmeier, and A. Geisselman, J. Magn. Magn. Mater. **177**, 748 (1997).

[16] O. Waldmann, J. Schülein, R. Koch, P. Müller, I. Bernt, R. W. Saalfrank, H. P. Andres, H. U. Güdel, and P. Allenspach, Inorg. Chem. **38**, 5879 (1999).

[17] W. Heisenberg, Z. f. Phys. **49**, 619 (1928).

[18] K. Binder and A. P. Young, Rev. Mod. Phys. **58**, 801 (1986).

[19] R. Boča, *Theoretical Foundations of Molecular Magnetism*, vol. 1 of *Current Methods in Inorganic Chemistry* (Elsevier, Amsterdam, 1999).

[20] T. Lis, Acta Chrytallogr. B **36**, 2042 (1980).

[21] L. Thomas, F. Lionti, R. Ballou, D. Gatteschi, R. Sessoli, and B. Barbara, Nature **383**, 145 (1996).

[22] Z. H. Jang, A. Lascialfari, F. Borsa, and D. Gatteschi, Phys. Rev. Lett. **84**, 2977 (2000).

[23] Y. Furukawa, K. Watanabe, K. Kumagai, F. Borsa, and D. Gatteschi, Phys. Rev. B **64**, 104401 (2001).

[24] L. Thomas and B. Barbara, J. Low Temp. Phys. **113**, 1055 (1998).

[25] N. Regnault, T. Jolicœur, R. Sessoli, D. Gatteschi, and M. Verdaguer, Phys. Rev. B **66**, 054409 (2002).

[26] G. Chaboussant, A. Sieber, S. Ochsenbein, H.-U. Güdel, M. Murrie, A. Honecker, N. Fukushima, and B. Normand, Phys. Rev. B **70**, 104422 (2004).

[27] C. A. Christmas, H. L. Tsai, L. Pardi, J. M. Kesselman, P. K. Gantzel, R. K. Chadha, D. Gatteschi, D. F. Harvey, and D. N. Hendrickson, J. Am. Chem. Soc. **115**, 12483 (1993).

[28] K. L. Taft, C. D. Delfs, G. C. Papaefthymiou, S. Foner, D. Gatteschi, and S. J. Lippard, J. Am. Chem. Soc. **116**, 823 (1994).

[29] A. Lascialfari, D. Gatteschi, F. Borsa, and A. Cornia, Phys. Rev. B **55**, 14341 (1997).

[30] A. Lascialfari, D. Gatteschi, F. Borsa, and A. Cornia, Phys. Rev. B **56**, 8434 (1997).

[31] M.-H. Julien, Z. Jang, A. Lascialfari, F. Borsa, M. Horvatić, A. Caneschi, , and D. Gatteschi, Phys. Rev. Lett. **83**, 227 (1999).

[32] G. L. Abbati, A. Caneschi, A. Cornia, A. C. Fabretti, and D. Gatteschi, Inorg. Chim. Acta **297**, 291 (2000).

[33] O. Waldmann, R. Koch, S. Schromm, J. Schülein, P. Müller, I. Bernt, R. W. Saalfrank, F. Hampel, and E. Balthes, Inorg. Chem. **40**, 2986 (2001).

[34] F. Meier and D. Loss, Phys. Rev. Lett. **86**, 5373 (2001).

[35] R. W. Saalfrank, I. Bernt, M. M. Chowdhry, F. Hampel, and G. B. M. Vaughan, Chem. Eur. J. **7**, 2765 (2001).

[36] A. Müller, M. Luban, C. Schröder, R. Modler, P. Kögerler, M. Axenovich, J. Schnack, P. C. Canfield, S. Bud'ko, and N. Harrison, Chem. Phys. Chem. **2**, 517 (2001).

[37] M. Axenovich and M. Luban, Phys. Rev. B **63**, 100407 (2001).

[38] A. Müller, E. Krickemeyer, S. K. Das, P. Kögerler, S. Sarkar, H. Bögge, M. Schmidt-mann, and S. Sarkar, Angew. Chem., Int. Ed. **39**, 1612 (2000).

[39] A. Müller, S. K. Das, E. Krickemeyer, P. Kögerler, H. Bögge, and M. Schmidtmann, Solid State Sciences **2**, 847 (2000).

[40] A. Müller, S. K. Das, , M. O. Talismanova, H. Bögge, P. Kögerler, M. Schmidtmann, S. S. Talismanov, M. Luban, and E. Krickemeyer, Angew. Chem., Int. Ed. **41**, 579 (2000).

[41] E. Ruiz, P. Alemany, S. Alvarez, and J. Cano, J. Am. Chem. Soc. **119**, 1297 (1997).

[42] E. Ruiz, J. Cano, S. Alvarez, and P. Alemany, J. Am. Chem. Soc. **120**, 11122 (1998).

[43] C. Calzado, J. Sanz, J. Malrieu, and F. Illas, Chem. Phys. Lett. **307**, 102 (1999).

[44] J. Kortus, C. S. Hellberg, and M. R. Pederson, Phys. Rev. Lett. **86**, 3400 (2001).

[45] M. R. Pederson, N. Bernstein, and J. Kortus, Phys. Rev. Lett. **89**, 097202 (2002).

[46] J. Kortus, T. Baruah, N. Bernstein, and M. R. Pederson, Phys. Rev. B **66**, 092403 (2002).

[47] O. Waldmann, Phys. Rev. B **61**, 6138 (2000).

[48] K. Bärwinkel, H.-J. Schmidt, and J. Schnack, J. Magn. Magn. Mater. **212**, 240 (2000).

[49] W. Feller, *An introduction to probability theory and its applications*, vol. 1 (John Wiley & Sons, New York, 1968), 3rd ed.

[50] D. Kouzoudis, J. Magn. Magn. Mater. **173**, 259 (1997).

[51] D. Kouzoudis, J. Magn. Magn. Mater. **189**, 366 (1998).

[52] J. Bonner and M. Fisher, Phys. Rev. **135**, A640 (1964).

[53] R. Botet and R. Jullien, Phys. Rev. B **27**, 631 (1983).

[54] K. Fabricius, U. Löw, K.-H. Mütter, and P. Ueberholz, Phys. Rev. B **44**, 7476 (1991).

[55] E. Manousakis, Rev. Mod. Phys. **63**, 1 (1991).

[56] O. Golinelli, T. Jolicœur, and R. Lacaze, Phys. Rev. B **50**, 3037 (1994).

[57] K. Fabricius, U. Löw, and J. Stolze, Phys. Rev. B **55**, 5833 (1997).

[58] C. Lanczos, J. Res. Nat. Bur. Stand. **45**, 255 (1950).

[59] J. K. Cullum and R. A. Willoughby, *Lánczos Algorithms for Large Symmetric Eigenvalue Computations*, vol. I (Birkhäuser, Boston, 1985).

[60] Z. Bai, J. Demmel, J. Dongarra, A. Ruhe, and H. van der Vorst, eds., *Templates for the Solution of Algebraic Eigenvalue Problems: A Practical Guide* (Society for Industrial & Applied Mathematics, Philadelphia, 2000).

[61] S. R. White, Phys. Rev. B **48**, 10345 (1993).

[62] I. Peschel, X. Wang, M. Kaulke, and K. Hallberg, eds., *Density-Matrix Renormalization* (Springer, Berlin, 1999).

[63] U. Schollwöck, Rev. Mod. Phys. (2004).

[64] S. R. White and D. Huse, Phys. Rev. B **48**, 3844 (1993).

[65] T. Xiang, Phys. Rev. B **58**, 9142 (1998).

[66] M. Exler and J. Schnack, Phys. Rev. B **67**, 094440 (2003).

[67] J. Schnack, H.-J. Schmidt, J. Richter, and J. Schulenburg, Eur. Phys. J. B **24**, 475 (2001).

[68] J. M. Radcliff, J. Phys. A: Gen. Phys. **4**, 313 (1971).

[69] A. Honecker, F. Meier, D. Loss, and B. Normand, Eur. Phys. J. B **27**, 487 (2002).

[70] W. Marshall, Proc. Royal. Soc. A (London) **232**, 48 (1955).

[71] E. H. Lieb, T. Schultz, and D. C. Mattis, Ann. Phys. (N.Y.) **16**, 407 (1961).

[72] E. H. Lieb and D. C. Mattis, J. Math. Phys. **3**, 749 (1962).

[73] M. Karbach, *Finite-Size-Effekte im eindimensionalen Spin-$\frac{1}{2}$-XXZ-Modell*, Ph.D. thesis, Bergische Universität - Gesamthochschule Wuppertal (1994).

[74] K. Bärwinkel, H.-J. Schmidt, and J. Schnack, J. Magn. Magn. Mater. **220**, 227 (2000).

[75] J. Schnack, Phys. Rev. B **62**, 14855 (2000).

[76] K. Bärwinkel, P. Hage, H.-J. Schmidt, and J. Schnack, Phys. Rev. B **68**, 054422 (2003).

[77] F. Haldane, Phys. Lett. A **93**, 464 (1983).

[78] F. Haldane, Phys. Rev. Lett. **50**, 1153 (1983).

[79] J. Schnack and M. Luban, Phys. Rev. B **63**, 014418 (2001).

[80] J. Schnack, M. Luban, and R. Modler, Europhys. Lett. **56**, 863 (2001).

[81] O. Waldmann, Phys. Rev. B **65**, 024424 (2002).

[82] B. Bernu, P. Lecheminant, C. Lhuillier, and L. Pierre, Phys. Rev. B **50**, 10048 (1994).

[83] M. Gross, E. Sánchez-Velasco, and E. D. Siggia, Phys. Rev. B **40**, 11328 (1989).

[84] J. Richter, Phys. Rev. B **47**, 5794 (1993).

[85] H.-J. Schmidt and M. Luban, J. Phys. A: Math. Gen. **36**, 6351 (2003).

[86] J. Schulenburg, A. Honecker, J. Schnack, J. Richter, and H.-J. Schmidt, Phys. Rev. Lett. **88**, 167207 (2002).

[87] H.-J. Schmidt, J. Phys. A: Math. Gen. **35**, 6545 (2002).

[88] J. R. Friedman, M. P. Sarachik, J. Tejada, and R. Ziolo, Phys. Rev. Lett. **76**, 3830 (1996).

[89] J. Tejada, J. M. Hernandez, and E. del Barco, J. Magn. Magn. Mater. **197**, 552 (1999).

[90] J. R. Friedman, V. Patel, W. Chen, S. K. Tolpygo, and J. E. Lukens, Nature **406**, 43 (2000).

[91] B. Barbara, I. Chiorescu, R. Giraud, A. G. M. Jansen, and A. Caneschi, J. Phys. Soc. Jpn. **69**, 383 (2000).

[92] F. Lionti, L. Thomas, R. Ballou, B. Barbara, A. Sulpice, R. Sessoli, and D. Gatteschi, J. Appl. Phys. **81**, 4608 (1997).

[93] P. Politi, A. Rettori, F. Hartmann-Boutron, and J. Villain, Phys. Rev. Lett. **75**, 537 (1995).

[94] A. L. Burin, N. V. Prokofev, and P. C. E. Stamp, Phys. Rev. Lett. **76**, 3040 (1996).

[95] P. Politi, A. Rettori, F. Hartmann-Boutron, and J. Villain, Phys. Rev. Lett. **76**, 3041 (1996).

[96] I. Chiorescu, R. Giraud, A. G. M. Jansen, A. Caneschi, and B. Barbara, Phys. Rev. Lett. **85**, 4807 (2000).

[97] A. Garg, Phys. Rev. B **64**, 094413 (2001).

[98] A. Garg, Phys. Rev. B **64**, 094414 (2001).

[99] C. S. Park and A. Garg, Phys. Rev. B **65**, 064411 (2002).

[100] H. A. De Raedt, A. H. Hams, V. V. Dobrovitski, M. Al-Saqer, M. I. Katsnelson, and B. N. Harmon, J. Magn. Magn. Mater. **246**, 392 (2002).

[101] O. Waldmann, Europhys. Lett. **60**, 302 (2002).

[102] L. D. Landau, Phys. Z. Sowjetunion **2**, 46 (1932).

[103] C. Zener, Proc. R. Soc. London, Ser. A **137**, 696 (1932).

[104] E. C. G. Stückelberg, Helv. Phys. Acta **5**, 369 (1932).

[105] H. D. Raedt, S. Miyashita, K. Saito, D. Garca-Pablos, and N. Garca, Phys. Rev. B **56**, 11761 (1997).

[106] W. Wernsdorfer, R. Sessoli, A. Caneschi, D. Gatteschi, A. Cornia, and D. Mailly, J. Appl. Phys. **87**, 5481 (2000).

[107] W. Wernsdorfer, N. Aliaga-Alcalde, D. N. Hendrickson, and G. Christou, Nature **416**, 406 (2002).

[108] R. Schenker, M. N. Leuenberger, G. Chaboussant, H. U. Gudel, and D. Loss, Chem. Phys. Lett. **358**, 413 (2002).

[109] O. Waldmann, R. Koch, S. Schromm, P. Müller, I. Bernt, and R. W. Saalfrank, Phys. Rev. Lett. **89**, 246401 (2002).

[110] A. J. Leggett, S. Chakravarty, A. T. Dorsey, M. P. A. Fisher, A. Garg, and W. Zwerger, Rev. Mod. Phys. **59**, 1 (1987).

[111] W. F. Giauque and D. MacDougall, Phys. Rev. **43**, 768 (1933).

[112] M. E. Zhitomirsky, Phys. Rev. B **67**, 104421 (2003).

[113] L. J. Zhu, M. Garst, A. Rosch, and Q. M. Si, Phys. Rev. Lett. **91**, 066404 (2003).

[114] M. E. Zhitomirsky and A. Honecker, J. Stat. Mech.: Theor. Exp. p. P07012 (2004).

[115] O. Derzhko and J. Richter, Phys. Rev. B **70**, 104415 (2004).

[116] J. Richter, J. Schulenburg, A. Honecker, J. Schnack, and H.-J. Schmidt, J. Phys.: Condens. Matter **16**, S779 (2004).